Am J Cancer Res 2026;16(1):291-313
www.ajcr.us /ISSN:2156-6976/ajcr0168605

Original Article

Restoring osimertinib sensitivity in EGFR-mutant NSCLC: the role of anlotinib in modulating Wnt/β-catenin/YAP pathways

Xuquan Jing[1,2*], Jiling Niu[3*], Li Li[4], Xiaoyang Zhai[2], Qinhao Xu[2], Zhongyu Shi[2], Yujie Wang[2], Hui Zhu[1,2#], Jinming Yu[1,2#]

[1]Shandong University Cancer Center, Jinan 250117, Shandong, China; [2]Department of Radiation Oncology, Shandong Cancer Hospital and Institute, Shandong First Medical University and Shandong Academy of Medical Sciences, Jinan 250117, Shandong, China; [3]Department of First Clinical Medical College, Shandong University of Traditional Chinese Medicine, Jinan 250014, Shandong, China; [4]Department of Oncology, Affiliated Hospital of Southwest Medical University, Luzhou 646000, Sichuan, China. [*]Equal contributors. [#]Co-corresponding authors.

Received September 6, 2025; Accepted January 13, 2026; Epub January 15, 2026; Published January 30, 2026

Abstract: This study investigated the role of anlotinib in restoring osimertinib sensitivity in EGFR-mutant non-small cell lung cancer (NSCLC) by targeting the Wnt/β-catenin/YAP signaling and PD-L1 expression. Using osimertinib-resistant HCC827 cells with high PD-L1 expression, a stable PD-L1 knockdown line (Sh-PD-L1) was generated through lentiviral vectors. Resistance was induced by stepwise exposure to osimertinib, and the two constructed resistant cell lines were named OR (osimertinib-resistant) and Sh-PD-L1-OR (PD-L1 knockdown osimertinib-resistant) cell lines. Functional assays, including wound healing, Transwell, and MTT, along with Western blot analysis, were conducted in both cell and animal models. Sh-PD-L1 significantly reduced PD-L1 and EGFR expression ($P < 0.001$), decreased cell viability, and lowered IC50 values compared to parental cells ($P < 0.001$). In OR, PD-L1 expression was elevated, and PD-L1 knockdown in the Sh-PD-L1-OR group reduced both PD-L1 and EGFR levels ($P < 0.001$), enhanced YAP inhibition, and reversed Wnt/β-catenin signaling activation ($P < 0.05$). Anlotinib treatment reduced cell viability, migration, and invasion, with enhanced effects in the Sh-PD-L1-OR group ($P < 0.001$). It decreased p-EGFR, PD-L1, and YAP expression while activating GSK3β and reducing β-catenin phosphorylation ($P < 0.05$). In vivo, anlotinib reduced tumor growth in Sh-PD-L1-OR models ($P < 0.01$), with decreased expression of EGFR, PD-L1, YAP, and β-catenin. These findings suggest that high PD-L1 expression promotes osimertinib resistance through activation of YAP and Wnt/β-catenin, and that anlotinib combined with osimertinib can reverse resistance by restoring GSK3β activity, activating the Hippo pathway, and inhibiting β-catenin signaling.

Keywords: Osimertinib resistance, PD-L1 expression, YAP signaling, Wnt/β-catenin pathway, anlotinib, combination therapy

Introduction

Lung cancer remains one of the leading causes of mortality worldwide, with non-small cell lung cancer (NSCLC) accounting for approximately 85% of all cases [1, 2]. Despite advances in treatment, the overall survival rate remains low, particularly among patients diagnosed at advanced stages [3, 4]. Currently, surgery, chemotherapy, and radiotherapy are the primary therapeutic options for NSCLC, while targeted therapies have gained prominence for patients with specific mutations [2]. Among these, third-generation epidermal growth factor receptor (EGFR) tyrosine kinase inhibitors (TKIs), such as osimertinib (AZD9291), have replaced first-generation EGFR-TKIs (gefitinib and erlotinib) as the standard first-line treatment for metastatic EGFR-mutant NSCLC [5, 6]. However, the emergence of acquired resistance to EGFR-TKIs remains a major barrier to effective treatment. Known mechanisms of resistance include the T790M mutation in the EGFR gene, which impairs the binding of third-generation EGFR-TKIs, MET amplification, and additional EGFR mutations [5, 6]. Additionally, epithelial-to-mes-

https://doi.org/10.62347/HSLI4871

enchymal transition (EMT) and the activation of bypass signaling pathways, such as the PI3K/AKT, MAPK, and Wnt/β-catenin pathways, have also been implicated in resistance [7]. Despite the development of next-generation EGFR-TKIs like osimertinib, overcoming resistance continues to present a significant clinical challenge, and new therapeutic strategies are urgently needed.

The relationship between EGFR signaling and the PD-L1/PD-1 axis has been explored, with studies showing that mutant EGFR signaling can enhance PD-L1 expression in cancer cells [8, 9]. Increased PD-L1 expression has been observed in lung cancer samples from EGFR-mutant patients [10, 11]. Our findings demonstrated that PD-L1 expression levels significantly impacted progression-free survival (PFS) [12]. Specifically, patients with strong PD-L1 expression (≥ 50%) had a significantly shorter median PFS compared to those with weak PD-L1 expression, although PD-L1 negativity was not associated with a poor prognosis [12]. This study suggests that higher PD-L1 expression in tumor cells may contribute to earlier progression and worse outcomes in EGFR-mutant NSCLC patients treated with third-generation EGFR-TKIs. However, the molecular mediator linking EGFR signaling to PD-L1 remains unclear.

Overexpression of PD-L1 has been associated with increased cell proliferation and chemotherapy resistance, independent of PD-1 and cytotoxic T cells [11, 13]. In this context of resistance, immunotherapy targeting immune checkpoints, such as PD-L1/PD-1, has recently garnered significant attention [2, 14, 15]. Unlike traditional chemotherapy, which primarily targets cancer cells, immunotherapy influences the tumor microenvironment, including immune cells, offering a potential treatment option for patients with chemoresistant lung cancer [16]. However, in NSCLC patients treated with anti-PD-1/PD-L1 immune checkpoint inhibitors (ICI), the incidence of grade 3 and higher toxicity ranges from 7-13% [17], although the incidence of adverse reactions remains considerably lower than that associated with chemotherapy [18]. Despite these advancements, significant limitations remain in all of these treatment strategies, often due to drug resistance, low efficacy, or severe side effects, which result in poor outcomes for patients with NSCLC.

Anlotinib (AL3818) is an oral multitargeted receptor TKI that targets several receptors, including vascular endothelial growth factor receptor (VEGFR), platelet-derived growth factor receptor (PDGFR), fibroblast growth factor receptor (FGFR), c-Kit, c-MET, and Ret [19-21]. The ALTER 0303 randomized phase III clinical trial showed that anlotinib significantly improved PFS and overall survival (OS) in 439 Chinese patients with advanced NSCLC, leading to its approval as a third-line treatment option for these patients in China [21]. Moreover, combining anlotinib with other therapeutic modalities has shown enhanced anticancer efficacy compared to monotherapy [22, 23]. Combination treatments, including chemotherapy, immunotherapy, and radiotherapy, have yielded improved outcomes [24-27]. Specifically, anlotinib combined with gefitinib has been reported to produce synergistic antitumor effects [28]. Studies on the combination of osimertinib and anlotinib to overcome drug resistance have shown that the two drugs can restore the sensitivity of resistant NSCLC cells and xenografts to osimertinib by inhibiting AXL phosphorylation and disrupting the c-MET/MYC/AXL axis [29]. Notably, anlotinib combined with PD-1 blocker enhanced the immune microenvironment and significantly inhibited tumor growth, showing superior efficacy compared to treatment alone [2]. Anlotinib enhances the tumor immune microenvironment by promoting CD8+ T cell dominance, with CCL5-mediated recruitment of CD8+ T cells playing a crucial role [2].

Although previous studies have highlighted the potential of combining anlotinib with EGFR-TKIs to overcome resistance, the mechanisms underlying this combination, particularly in relation to PD-L1 expression and its modulation, remain unclear. This study aims to investigate how anlotinib restores osimertinib sensitivity in EGFR-mutant NSCLC by inhibiting key signaling pathways and modulating PD-L1 expression. Understanding these mechanisms will provide insights into novel therapeutic strategies to overcome acquired resistance in advanced NSCLC, potentially improving patient outcomes and offering a more effective treatment approach.

Methods

Cell lines

In our previous research, we found that 54% of NSCLC patients had exon 19 deletions in EGFR,

while 46% had the exon 21 L858R mutation, with 65.33% of patients undergoing osimertinib treatment [12]. The wild-type cell line H1993 and A549, along with the EGFR-mutant cell lines H1975 (T790M and L858R mutation) and HCC827 (exon 19 deletion), were obtained from the American Type Culture Collection (ATCC, Manassas, VA, USA) and the Institute of Biochemistry and Cell Biology, Chinese Academy of Sciences (Shanghai, China), respectively. The H1993, PC-9, H1975, and HCC827 cell lines were cultured in RPMI 1640 medium (Thermo Fisher, 11875093), supplemented with 10% fetal bovine serum (FBS; Thermo Fisher, 16000044), 100 μg/mL penicillin (Thermo Fisher, 15140122), and 0.1 mg/mL streptomycin, and maintained in a 37°C incubator with a 5% CO_2 atmosphere.

Stable transfection

To establish a PD-L1 knockdown stable cell line, two DNA fragments corresponding to PD-L1 shRNA-1 (5'-GCATTTGCTGAACGCATTTAC-3') and PD-L1 shRNA-2 (5'-CGAATTACTGTGAAAGTCAAT-3') were cloned into the lentiviral vector pGLV2-U6-Puro (GenePharma, Shanghai, China), which contains BamHI and EcoRI restriction sites. A control shRNA sequence was used as a negative control. The PD-L1 knockdown construct (Sh-PD-L1) or the control vector was co-transfected with packaging plasmids into 293T cells using Lipofectamine 2000 (Invitrogen, 11668027). After 48 h, lentivirus particles were harvested, filtered through a 0.45 μm PVDF filter, and used to infect target cells. Infected cells were cultured for an additional 48 h and subsequently subjected to puromycin (Sigma-Aldrich, P8833) selection at concentrations ranging from 0.4 μg/mL to 2 μg/mL. PD-L1 knockdown efficiency was confirmed by RNA and protein analyses.

To construct a stable GSK3β overexpression cell line in OR (osimertinib-resistant) cells, the GSK3β coding sequence was cloned into the pLVX-IRES-Neo vector and transfected into human embryonic kidney 293T cells along with packaging plasmids using Lipofectamine 2000. The empty vector was used as a negative control. The cells were incubated in DMEM (Thermo Fisher, 11995073) supplemented with 10% FBS in a humidified 5% CO_2 incubator at 37°C for 48 h. After incubation, the lentiviral supernatant was collected and used to infect OR cells. Two days post-infection, stable cells were selected with 400 μg/mL G418 (Amresco, Solon, 97223).

Osimertinib resistance induction

Osimertinib (10 Mm; Selleck Chemicals, S7788) was dissolved in DMSO, ensuring that the final DMSO (Sigma-Aldrich, D8418) concentration in both the drug-treated and control media was less than 1%. HCC827 cells were seeded at a density of approximately 1×10^6 cells per well and treated with 5 μM osimertinib for 24 h. Once the cells reached 80-90% confluence, the osimertinib concentration gradually increased in subsequent rounds of treatment, and the exposure time was extended to 72 h. The final osimertinib concentration was 10 μM. This process continued for several weeks, during which the cells were cultured in medium containing 5-10 μM osimertinib for a total of 5 weeks. After 5 weeks, total RNA was extracted, and PD-L1 gene expression was detected by flow cytometry, while PD-L1 and EGFR protein expression were assessed by western blot (WB). This method was used to establish both OR (osimertinib-resistant) and Sh-PD-L1-OR (PD-L1 knockdown osimertinib-resistant) cell lines.

Wound healing assay

HCC827 cells were seeded in 6-well plates until reaching 80-90% confluence. A straight scratch was made using a 200 μL pipette tip. Images were captured at 0, 24, 48 and 72 h to assess cell migration rates.

Transwell migration and invasion assays

Migration and invasion abilities of the cells were assessed using 24-well Transwell chambers (Corning, USA). For the migration assay, 5×10^4 cells were seeded into the upper chamber, with 0.4 mL of serum-free medium in the upper compartment. The lower chamber was filled with 0.6 mL of medium containing 20% FBS. After incubating for 24 h at 37°C, cells were fixed with methanol for 15 min and stained with 0.1% crystal violet (Sigma-Aldrich, USA) for 30 min. The stained cells were washed with water, and the membrane was mounted on a glass slide for microscopic analysis. The experiment was performed in triplicate.

For the invasion assay, the upper chamber and insert of the 24-well Transwell system (Corning, USA) were coated with Matrigel (BD Biosciences, 354234) at a 1:7 dilution ratio prior to cell seeding. After allowing the Matrigel to solidify at 37°C for 2 h, approximately 6×10^4 cells (transfected group) and 10×10^4 cells (control group) were seeded in the upper chamber, and the lower chamber was filled with medium containing 20% FBS as a chemoattractant. The cells were incubated for 24 h at 37°C. After incubation, the non-invasive cells on the upper surface of the membrane were gently removed with a cotton swab. The invasive cells on the lower surface of the membrane were fixed with 4% paraformaldehyde for 20 min, followed by staining with hematoxylin for 10 min. Invasive cell numbers were counted by randomly selecting five high-power fields (200× magnification) under a light microscope. The experiment was performed in triplicate.

MTT assay for cell viability

HCC827 cells were seeded at 2×10^3 cells per well in 96-well plates. After 24 h, cells were treated with varying concentrations of osimertinib (0-15 μM) for 96 h. Post-treatment, the cells were washed with PBS, and 20 μL of MTT (5 mg/mL) was added to each well, followed by a 4-hour incubation at 37°C. Dimethyl sulfoxide (DMSO, 150 μL) was added to dissolve formazan crystals, and absorbance was measured at 570 nm. Cell viability was calculated relative to control, and IC50 values were determined using non-linear regression analysis.

Apoptosis analysis

Apoptosis was assessed in four groups of HCC827 cells using 7-AAD staining in combination with Annexin V-FITC. Cells were incubated with Annexin V-FITC and 7-AAD (Yeasen, 403-11ES50) according to the manufacturer's protocol to differentiate early apoptotic, late apoptotic, and necrotic cells. Apoptosis was evaluated by flow cytometry on a BD FACSCalibur flow cytometer. For each group, the percentage of early apoptotic (Annexin V-FITC positive, 7-AAD negative) and late apoptotic (Annexin V-FITC positive, 7-AAD positive) populations were quantified. Cell viability was assessed by 7-AAD staining (7-AAD positive cells) to distinguish necrotic cells. Data was collected and analyzed using FlowJo software (Tree Star, Inc.) to determine the apoptosis rate in each group, comparing pre- and post-resistance conditions. Statistical analysis was performed to evaluate the significance of apoptosis changes between the treatment groups.

Xenograft models

All experimental animals were obtained from the Beijing Vital River Laboratory Animal Technology Co., Ltd. (Beijing, China) and housed under specific pathogen-free conditions (22 ± 2°C, 55 ± 10% humidity, 12-h light/dark cycle) with ad libitum access to food and water. Male BALB/c nude mice (4-6 weeks old) were subcutaneously injected with 5×10^6 HCC827/OR or PD-L1 knockdown cells suspended in PBS.

Mice were randomly divided into four groups (n = 5 per group) once tumors reached 70-100 mm^3: (1) NC (HCC827), (2) OR (3) Sh-PD-L1, and (4) Sh-PD-L1-OR. Mice received daily gavage of control (1% DMSO), anlotinib (1.5 mg/kg) therapy for 16 days. Tumor volumes were calculated as $V = L\times W^2/2$, and on day 21, mice were euthanized under deep anaesthesia using an intraperitoneal injection of sodium pentobarbital (150 mg/kg), followed by cervical dislocation to confirm death, for tissue collection and metastasis assessment.

Immunohistochemistry (IHC)

Tumor sections were deparaffinized, rehydrated, and subjected to antigen retrieval using citrate buffer (pH 6.0). Sections were incubated overnight at 4°C with primary antibodies against PD-L1 and β-catenin (1:400). DAB was used for visualization, and hematoxylin was applied for counterstaining. Staining intensity and the percentage of positively stained cells were scored to evaluate protein expression.

Hematoxylin and Eosin (H&E) staining

Tissue sections were deparaffinized, rehydrated, and stained with hematoxylin for 5 min. After differentiation with acid alcohol, sections were blued with ammonia water, counterstained with eosin, dehydrated, and mounted for microscopic evaluation.

Western blot analysis

Total protein was extracted from HCC827 cells treated with or without osimertinib (0 μM, 1 μM,

or 10 μM) for 48 h. Proteins were quantified using the BCA assay, separated via SDS-PAGE, and transferred to PVDF membranes. Membranes were incubated with primary antibodies against EGFR, phosphorylated EGFR, PD-L1, and β-catenin, followed by HRP-conjugated secondary antibodies. Bands were visualized using ECL reagents and quantified with imaging software, normalized to β-actin levels.

Co-immunoprecipitation (CO-IP) of protein-protein interactions

For the detection of protein-protein interactions, OR cells and sh-PD-L1 cells were transfected with or without HA-β-catenin, Flag-YAP2, and Flag-TAZ. Cells were seeded at 25% confluence (Day 0) and transfected with siRNA for 8 hours or DNA for 24 hours, followed by medium replacement. After 48 h (Day 3), cells were harvested. Cells were lysed in a buffer containing 20 mM HEPES (pH 7.8), 400 mM KCl, 5 mM EDTA, 0.4% NP40, 5% glycerol, and protease and phosphatase inhibitors, followed by sonication. The lysates were clarified by centrifugation. For immunoprecipitation, the extracts were diluted in binding buffer (20 mM HEPES, pH 7.8, 100 mM NaCl, 5% glycerol, 2.5 mM $MgCl_2$, 1% Triton X-100, 0.5% NP40) and incubated overnight at 4°C with anti-HA antibody (Sigma), anti-Flag antibody (Sigma), or anti-tubulin antibody (Santa Cruz). The immunocomplexes were then bound to protein G-agarose beads. After washing four times with cold binding buffer, the immune complexes were resuspended in SDS sample buffer and analyzed by SDS-PAGE and WB.

For IgG IP and α-YAP IP, the lysates were immunoprecipitated with either control rabbit IgG or anti-YAP antibody (Santa Cruz, sc-101199), followed by detection of β-catenin (α-β-catenin) and YAP (α-YAP) by WB.

To assess the role of phosphorylation in YAP signaling, cells were treated with or without HA-GSK3β (Purchased from Baosai Biotech). The phosphorylation levels of YAP were detected by WB using the following antibodies: anti-HA (α-HA), anti-phospho-YAP (Ser127) (α-pYAP), and anti-YAP (α-YAP). The analysis was performed to evaluate changes in YAP phosphorylation status upon treatment. For pulldown assays, cells were lysed and subjected to pulldown using GST or GST-β-catenin. The interaction between phosphorylated YAP and β-catenin was evaluated by detecting the following proteins: anti-pYAP (Ser127) (α-pYAP), anti-GST (α-GST), and anti-GST-β-catenin (α-GST-β-catenin) through WB. The pulldown efficiency and binding interactions were determined by comparing the expression levels of these proteins.

For phospho-specific assays, cells were treated with or without HA-GSK3β and lysed in the same buffer as above. For immunoprecipitation, the lysates were incubated with anti-HA (Sigma), anti-Flag (Sigma), or anti-Myc (Santa Cruz, 9E10 sc-40) resin for 4 h at 4°C. Immunocomplexes were washed three times with cold binding buffer, resuspended in SDS sample buffer, and analyzed by SDS-PAGE and WB.

Quantitative real-time PCR (qRT-PCR)

Total RNA was extracted from tumor tissues and HCC827 cells using the Bio-Rad RNA extraction kit, following the manufacturer's protocol. RNA purity and concentration were measured at 260/280 nm using a spectrophotometer. cDNA was synthesized from 2 μg of total RNA using the iScript cDNA Synthesis Kit. qRT-PCR was performed with SYBR Green Supermix on a CFX Connect RT-PCR system using specific primers for EGFR, PD-L1, β-catenin, E-cadherin, N-cadherin, Vimentin and β-actin (**Table 1**).

For the qRT-PCR reaction, the total reaction volume was 20 μL, containing 10 μL of SYBR Green Supermix, 0.4 μL of forward primer (10 μM), 0.4 μL of reverse primer (10 μM), 1 μL of cDNA template, and 8.2 μL of nuclease-free water. The amplification was carried out with an initial denaturation at 95°C for 2-3 min, followed by 40 cycles of 95°C for 10-15 s and 60°C for 30-45 s. A melt curve analysis was performed from 65°C to 95°C in increments of 0.5°C to confirm primer specificity. Gene expression was normalized to β-actin using the $2^{-\Delta\Delta Ct}$ method. Each sample was analyzed in triplicate.

Reagents

Anlotinib, an investigational drug under study for its potential to reverse osimertinib resistance, was provided by Chia Tai Tianqing Pharmaceutical Co., Ltd. (Jiangsu, China). IWR-1-endo, a Wnt signaling inhibitor used in the

Table 1. qRT-PCR primer sequences for target genes

Gene	Forward Primer (5'-3')	Reverse Primer (5'-3')
EGFR	AACACCCTGGTGTGTGGAAGTACG	TCGTTGGACAGCCTTCAAGACC
PD-L1	CCTACTGGCATTTGCTGAACGCAT	ACCATAGCTGATCATGCAGCGGTA
β-catenin	TCCTGAGGAAGAGGATGTGGAT	CCTCTGAGCTCGAGTCATTGC
E-cadherin	ACCATTAACAGGAACACAGG	CAGTCACTTTCAGTGTGGTG
N-cadherin	TTGAGCCTGAAGCCAACCTT	TGTAGGTGGCCACTGTGCTTAC
Vimentin	CGCCAACTACATCGACAAGGTGC	CTGGTCCACCTGCCGGCGCAG
β-actin	TCCTGTGGCATCCACGAAACT	GAAGCATTTGCGGTGGACGAT

study, induces Axin2 protein levels and promotes beta-catenin phosphorylation by stabilizing the Axin skeleton destruction complex, purchased from Selleckchem (S7086, Houston, TX, USA). XAV939 is a small molecule inhibitor that selectively inhibits tankyrase 1 and 2 (TNKS 1/2) activity, purchased from Sigma-Aldrich (Catalog No. X3004). TRULI, a LAST pathway inhibitor, was purchased from MedChemExpress (HY-138489, Monmouth Junction, NJ, USA). Verteporfin, a YAP/TEAD signaling pathway inhibitor, was purchased from Sigma-Aldrich (SML0534, St. Louis, MO, USA). EGF Recombinant Protein, used as an EGF agonist in the study, was purchased from Sigma-Aldrich (St. Louis, MO, USA). Dimethyl sulfoxide (DMSO) was used to dissolve these drugs, and the resulting solutions were stored at -20°C until further use in experimental procedures.

The following primary antibodies were used for WB and IHC: anti-EGFR (Bio-Techne, AF1280, RRID: AB_354717), anti-p-EGFR (Y1068) (R&D Systems, MAB3570), anti-PD-L1 (Proteintech, 66248-1-Ig), anti-β-catenin (Santa Cruz Biotechnology, sc-7963), anti-YAP (Cell Signaling Technology, #14074), anti-p-YAP (Ser127) (CST, #13008), anti-β-actin (CST, #4970), anti-LATS1 (CST, #3477), anti-p-LATS1 (Ser909) (CST, #9157), anti-MOB1 (CST, #33863), anti-p-MOB1 (CST, #8699), Anti-rabbit IgG (HRP) (CST, #7074)

Statistical analysis

All experiments were performed in independent triplicates. Quantitative data are expressed as mean ± standard deviation (SD). Statistical analyses were executed using GraphPad Prism 10.4.2 software. Comparisons between two groups were performed using the Student's t-Test. For comparisons among multiple groups, one-way analysis of variance (ANOVA) was employed, followed by Tukey's post hoc test for pairwise comparisons. For data analyzed across multiple time points, repeated measures ANOVA was utilized with Bonferroni's post hoc adjustment. A *P*-value of less than 0.05 was defined as statistically significant (*$P < 0.05$, **$P < 0.01$, ***$P < 0.001$).

Results

Impact of PD-L1 knockdown on EGFR signaling and osimertinib resistance

In our study, compared to the parental wild-type cell lines H1993 and A549, the mRNA levels of PD-L1 were significantly higher in the HCC827 (exon 19 del) and H1975 (T790M, L858R) cell lines (**Figure 1A**, All $P < 0.001$). We selected the PD-L1 high-expressing HCC827 cell line as a control group for further analysis, consistent with previous studies. To simulate the clinical scenario of low PD-L1 expression, we knocked down PD-L1 in the HCC827 cells. The experimental groups included NC (HCC827 control), Sh-PD-L1 (PD-L1 knockdown), and two osimertinib-resistant groups (OR and Sh-PD-L1-OR). Compared to the NC group, the Sh-PD-L1 group resulted in a significant reduction in both mRNA and protein expression levels of PD-L1 (**Figure 1B** and **1D**, $P < 0.001$). Surprisingly, following PD-L1 knockdown, the mRNA and protein expression levels of EGFR were also significantly decreased (**Figure 1C** and **1D**, $P < 0.001$).

The cell viability and IC50 values of all four groups were assessed using the MTT assay (**Figure 1E** and **1F**). To establish osimertinib resistance, we exposed HCC827 cells to increasing concentrations of osimertinib over five weeks. The results showed that at 10 μM, HCC827 cells began to acquire resistance, with increased cell viability and IC50 values com-

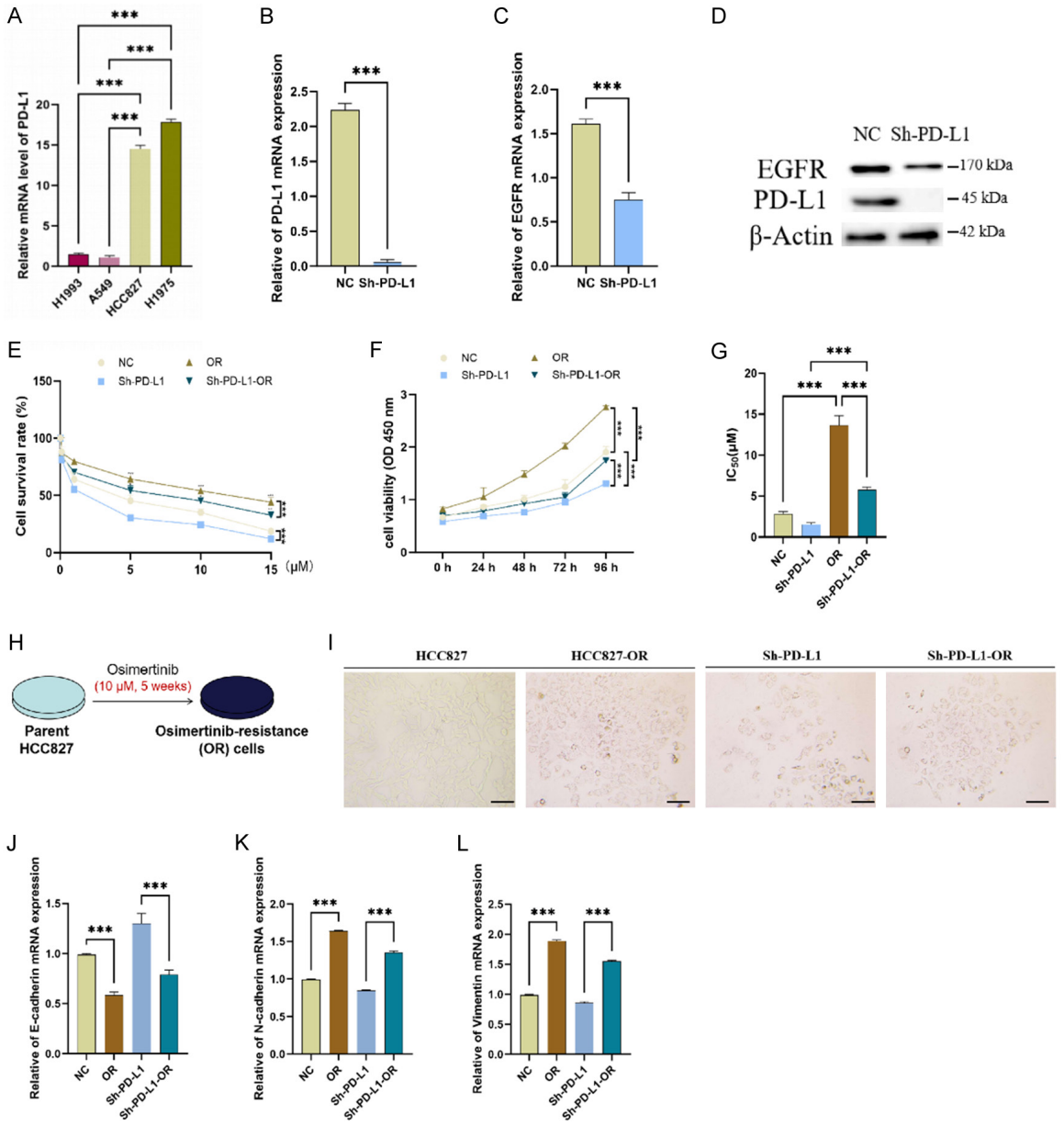

Figure 1. Impact of PD-L1 knockdown on EGFR signaling, osimertinib resistance, and EMT marker expression in HCC827 cells. A-D. PCR and Western blot showed the mRNA levels of PD-L1 and EGFR (epidermal growth factor receptor) in cells of each group. E-G. MTT was used to determine the cell survival rate, cell viability and IC50 value of cells in each group before and after drug resistance. H. Schematic diagram of cell resistance induced by osimertinib (5-10 μM, 5 weeks). I. Observe the morphological differences before and after drug resistance in each group under the microscope (Scale Bar: 100 μm; original magnification, ×200). J-L. mRNA expressions of E-cadherin, N-cadherin and Vimentin. *P < 0.05, **P < 0.01, ***P < 0.001.

pared to parental cells (P < 0.001, **Figure 1G**). The Sh-PD-L1 group showed reduced viability, suggesting that PD-L1 knockdown enhances survival in osimertinib. Interestingly, the Sh-PD-L1-OR exhibited a significant reduction in PD-L1 expression and a substantially lower IC50 value compared to the OR group (5.53 μM vs 12.35 μM, P < 0.001, **Figure 1H**).

Morphological changes, particularly the phenotypic transition (EMT), were observed and linked to acquired drug resistance [29]. High magnification microscopy was used to examine the morphological changes in HCC827 cells and their osimertinib-resistant derivatives. As shown in **Figure 1I**, the parental HCC827 cells maintained a typical epithelial morphology,

whereas the Sh-PD-L1 cells exhibited a more rounded and compact appearance. The OR cells were notably larger than their parental HCC827 counterparts, exhibiting fibroblast-like morphology, elongated spindle shapes, and an increased number of cells. In contrast to the OR group, the Sh-PD-L1-OR group showed significantly fewer cells, although typical spindle-shaped fibroblastic morphology was also observed following resistance induction.

Resistance-related markers showed that, compared to the NC group, the mRNA expression levels of E-cadherin were significantly increased in the Sh-PD-L1 group ($P < 0.001$), while the levels of N-cadherin and Vimentin were significantly reduced (both $P < 0.05$). Conversely, the OR group exhibited a significant increase in N-cadherin and Vimentin mRNA levels, with a marked decrease in E-cadherin expression ($P < 0.001$, **Figure 1J-L**). Notably, the Sh-PD-L1-OR group exhibited relatively lower expression of N-cadherin and Vimentin compared to the OR group, further supporting the hypothesis that the suppression of PD-L1 expression may mitigate resistance by modulating EMT-related marker expression.

PD-L1 upregulation promotes migratory, invasive, and anti-apoptotic phenotypes in osimertinib resistant cells

Cell migration before and after resistance was assessed using the Transwell assay (**Figure 2A**). Compared to the NC group, the Sh-PD-L1 group was significantly reduced migration ($P < 0.01$), whereas the OR group showed a marked increase in migration ($P < 0.001$). Notably, the Sh-PD-L1-OR group demonstrated a substantial decrease in migration compared to the OR group ($P < 0.001$), suggesting that PD-L1 plays a role in promoting migration in osimertinib-resistant cells. Similarly, the Transwell invasion assay revealed that the Sh-PD-L1 group exhibited significantly reduced invasiveness compared to the NC group ($P < 0.05$), while the OR group displayed a significant increase in invasiveness ($P < 0.01$, **Figure 2B**). Importantly, the Sh-PD-L1-OR group showed reduced invasiveness compared to the OR group ($P < 0.05$), indicating that PD-L1 knockdown inhibits the invasion potential of osimertinib-resistant cells.

Apoptosis before and after resistance was assessed by Annexin V/PI flow cytometry (**Figure 2C**). Compared to the NC group, the Sh-PD-L1 group showed a significant increase in both early and late apoptosis rates ($P < 0.001$). In resistant cells, both groups exhibited notable resistance to osimertinib-induced cell death compared to pre-resistance conditions ($P < 0.001$, $P < 0.01$), indicating the development of acquired resistance. In contrast, the Sh-PD-L1-OR group demonstrated significantly increased apoptosis ($P < 0.001$), indicating that PD-L1 knockdown may help restore the sensitivity of resistant cells to osimertinib.

Dynamic regulation of PD-L1 and EGFR in osimertinib resistance

To investigate the potential relationship between PD-L1 and EGFR in the context of osimertinib resistance, we first analyzed the TCGA COAD dataset via the GEPIA database. A significant correlation was observed between the expression levels of PD-L1 (CD274) and EGFR (**Figure 3A**, log2-transformed TPM values, $P = 0.034$), suggesting that these two molecules might be co-regulated in the development of resistance to osimertinib.

To induce resistance in the OR group, osimertinib was administered at concentrations of 5-10 μM over a period of approximately five weeks. As osimertinib concentration increased, sustained EGFR-TKI treatment led to significantly higher PD-L1 levels in the NC group compared to the Sh-PD-L1 group (**Figure 3B**). Further PCR analysis revealed that as osimertinib concentrations increased, EGFR mRNA expression was significantly elevated in both the OR and Sh-PD-L1-OR groups compared to the NC group ($P < 0.001$ for both, **Figure 3C**). WB analysis revealed elevated EGFR and p-EGFR levels in the OR cells, particularly at higher osimertinib concentrations (1 μM and 10 μM), indicating activated EGFR signaling linked to resistance (**Figure 3D**). Similarly, PD-L1 and p-PD-L1 expression were upregulated in the OR cells, suggesting PD-L1's involvement in maintaining resistance. Importantly, PD-L1 knockdown in the Sh-PD-L1-OR group significantly reduced both PD-L1 and EGFR expression, underscoring their reciprocal regulation. These findings imply that PD-L1 may modulate EGFR expression via phosphorylation, activating downstream survival pathways that contribute to osimertinib resistance. The

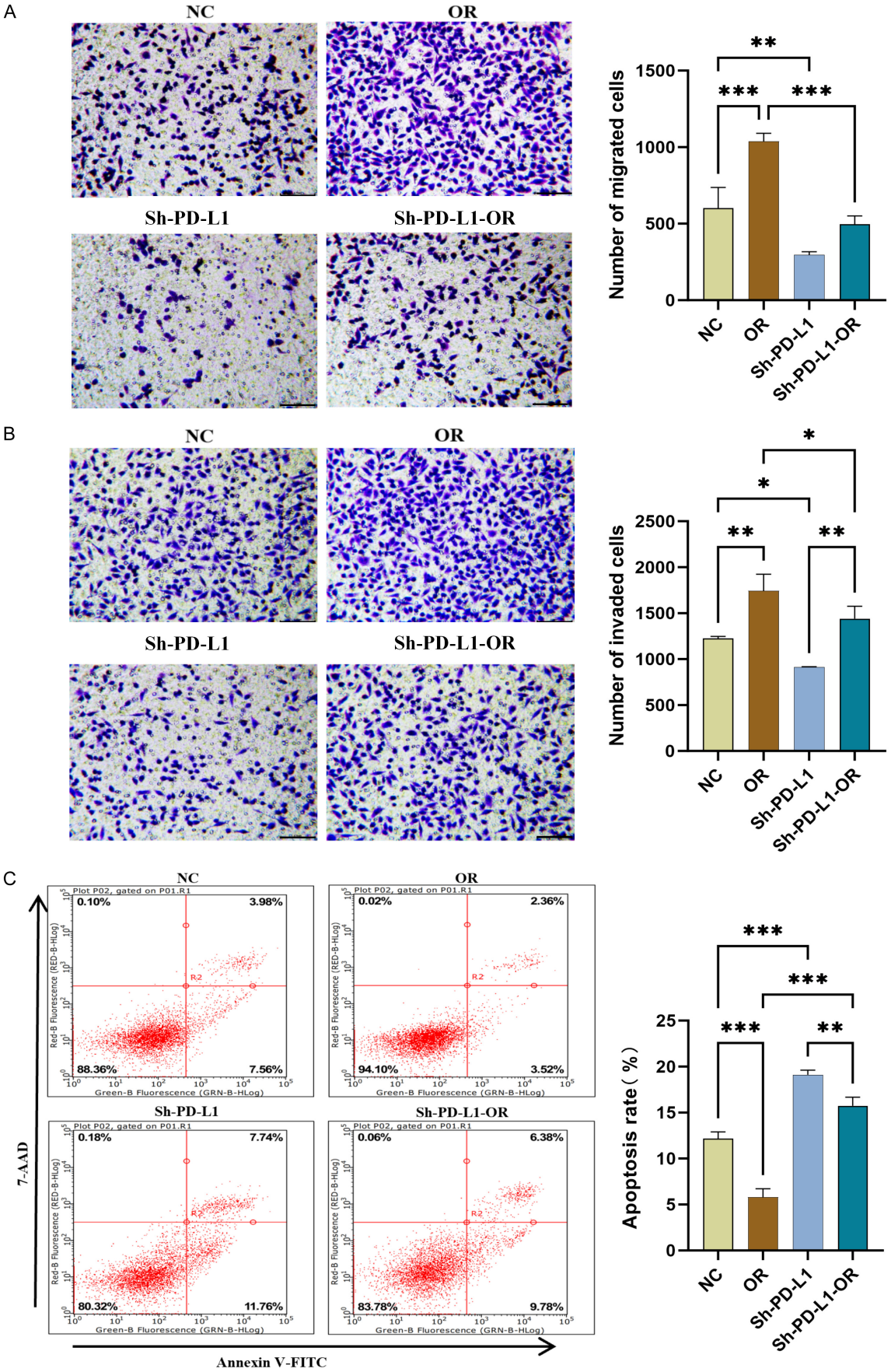
A
NC
OR
Sh-PD-L1
Sh-PD-L1-OR
Number of migrated cells
1500
1000
500
0
**
***
***
NC
OR
Sh-PD-L1
Sh-PD-L1-OR
B
NC
OR
Sh-PD-L1
Sh-PD-L1-OR
Number of invaded cells
2500
2000
1500
1000
500
0
*
*
**
**
NC
OR
Sh-PD-L1
Sh-PD-L1-OR
C
NC
OR
Sh-PD-L1
Sh-PD-L1-OR
Plot P02, gated on P01.R1
0.10%
3.98%
88.36%
7.56%
0.02%
2.36%
94.10%
3.52%
0.18%
7.74%
80.32%
11.76%
0.06%
6.38%
83.78%
9.78%
R2
Red-B Fluorescence (RED-B-HLog)
Green-B Fluorescence (GRN-B-HLog)
7-AAD
Annexin V-FITC
Apoptosis rate (%)
25
20
15
10
5
0
***
***
***
**
NC
OR
Sh-PD-L1
Sh-PD-L1-OR

Figure 2. The functional changes of cells in each group before and after drug resistance. A and B. Transwell migration assays were used to evaluate the migration and invasion abilities of cells in each group before and after osimertinib resistance (Scale Bar: 100 μm; original magnification, ×200). C. Annexin V/PI flow cytometry was used to analyze the apoptosis rate of cells in each group before and after osimertinib resistance. **P* < 0.05, ***P* < 0.01, ****P* < 0.001.

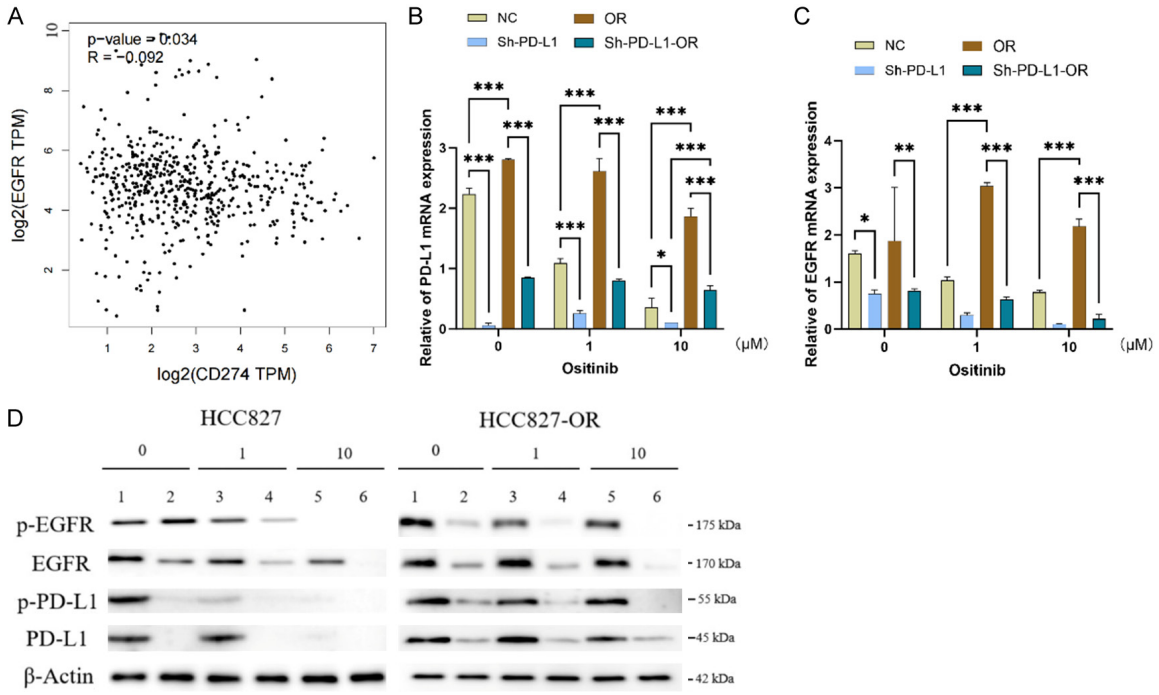

Figure 3. Each cell resistance before and after PD-L1 and the change of the EGFR gene and protein levels. (A) CD274 (PD-L1) and correlation analysis of EGFR. PCR analysis of PD-L1 and EGFR mRNA expression in osimertinib-resistant cells in groups (B) and (C) at different concentrations. (D) Western blot was used to analyze the protein expressions of p-EGFR, total EGFR, p-PD-L1 and PD-L1 in each group before and after drug resistance (1, 3, and 5 represent the addition of 0, 1, and 10 μM of osimertinib to NC respectively, and 2, 4, and 6 represent the addition of 0, 1, and 10 μM of osimertinib to Sh-PD-L1 respectively. The left cohort is before drug resistance, and the right one is after drug resistance). **P* < 0.05, ***P* < 0.01, ****P* < 0.001.

mechanistic link between PD-L1 and EGFR is likely mediated by the activation of downstream signaling pathways that modulate tumor cell survival and drug resistanc [30, 31].

The role of PD-L1 in modulating YAP activation and hippo pathway dysregulation in osimertinib-resistant cells

PD-L1 may directly regulate YAP transcription and its downstream signaling activity. Compared to the NC group, both YAP expression and phosphorylation levels were both upregulated in the OR group, consistent with elevated PD-L1 expression (**Figure 4A**). Additionally, the expression of Hippo pathway-related proteins LATS1 and MOB1 was elevated in the OR group compared to pre-resistance, although their phosphorylation levels were reduced. These results suggest that PD-L1 upregulation in drug-resistant cells may suppress downstream Hippo signaling by inhibiting LATS1/2 activity. This inhibition promotes YAP nuclear translocation and enhances its transcriptional activity.

In contrast, in the Sh-PD-L1-OR group, LATS1 and MOB1 expression levels were decreased, while their phosphorylation levels were elevated. Compared to the Sh-PD-L1 group, the Sh-PD-L1-OR group showed increased phosphorylation levels of LATS1 and MOB1, with no significant change in their dephosphorylation status. In summary, PD-L1 knockdown reversed these effects, indicating that PD-L1-induced drug resistance regulates Hippo signaling by modulating the phosphorylation status of its components.

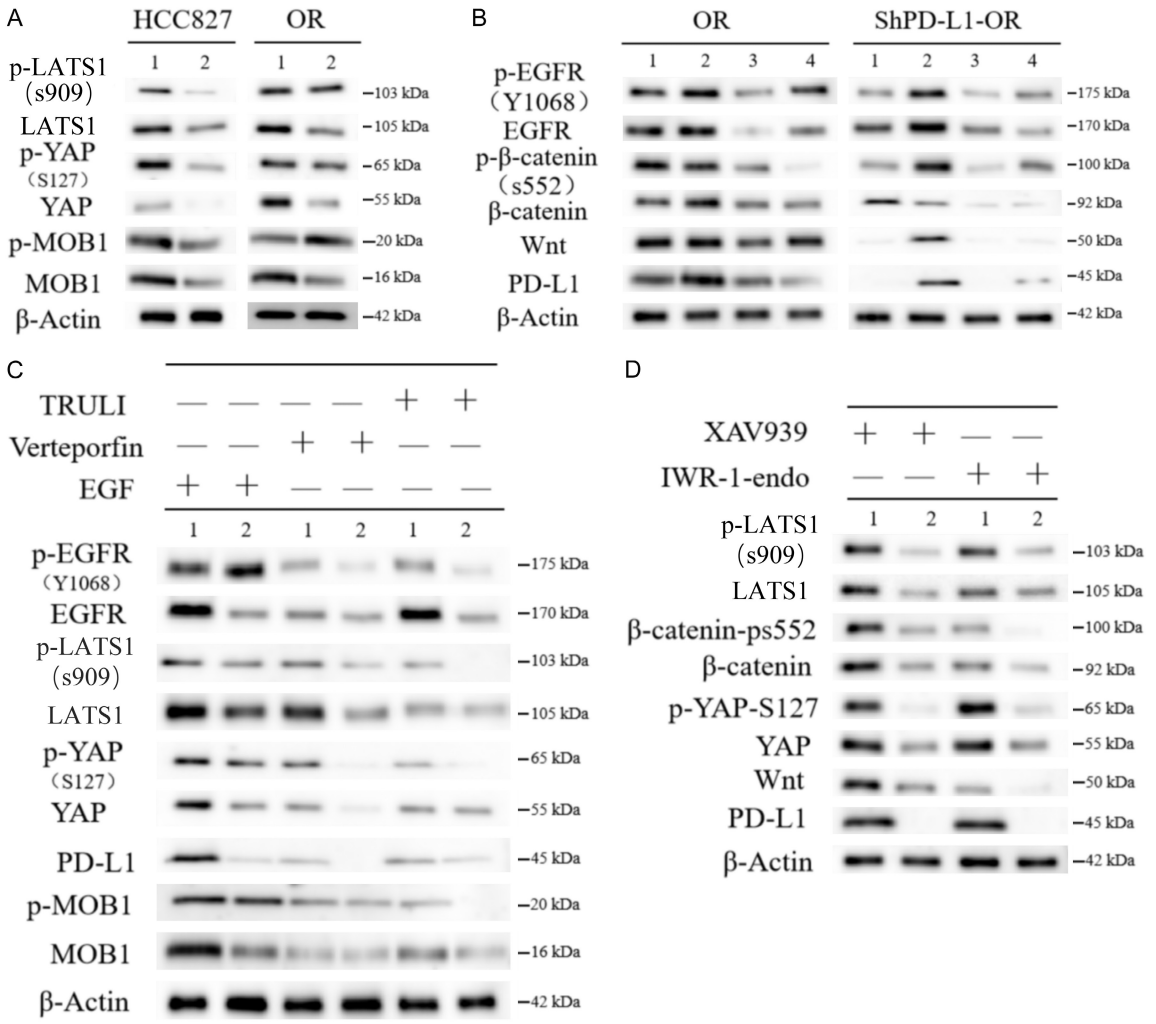

Figure 4. HCC827 resistance induces the closure of the Hippo pathway and the activation of the Wnt/β-catenin pathway. A. YAP Expression and Phosphorylation in NC (Negative control) and Sh-PD-L1 Groups (PD-L1 knockdown). Western blot analysis of YAP/MOB1/LATS1/2 pathway-related proteins was performed to assess changes in the expression and phosphorylation of YAP (1 and 2 represent NC and Sh-PD-L1 groups, respectively). B. EGF Stimulation Induces YAP Activation in OR (osimertinib-resistant) and Sh-PD-L1-OR (PD-L1 knockdown osimertinib-resistant) Groups (1 and 2 represent OR and Sh-PD-L1-OR groups, respectively). C. Wnt/β-Catenin Pathway Activation and Its Effect on PD-L1 Expression in Resistant Cells (1 NC group; 2 TGF agonist; 3 Wnt inhibitor; 4 β-catenin nuclear translocation inhibitors). D. YAP Inhibition Results in the Downregulation of the Hippo Pathway and the Upregulation of the Wnt/β-Catenin Pathway (1 and 2 represent OR and Sh-PD-L1-OR groups, respectively).

EGF stimulation promotes the transcription and protein expression of PD-L1 [32]. It was observed that the protein expressions of PD-L1 and P-EGFR in the two drug resistant groups increased upon EGF treatment (**Figure 4B**). EGF activation resulted in increased phosphorylation levels of EGFR, YAP, LATS1, and MOB1, with the OR group showing higher levels than the Sh-PD-L1 group. After the addition of Verteporfin, the Sh-PD-L1-OR group displayed a more significant reduction in YAP expression compared to the OR group. Although the expression of LATS1 in the OR group remained unchanged, its phosphorylation level decreased, and MOB1 dephosphorylation was also reduced. In contrast, the Sh-PD-L1-OR group exhibited a more pronounced inhibition of downstream signaling proteins. Interestingly, Verteporfin not only significantly reduced YAP expression and phosphorylation in the OR group but also notably decreased the expression and phosphorylation of EGFR. Similarly, following

TRULI treatment, all downstream signals were inhibited, except for EGFR expression.

In conclusion, PD-L1 upregulation in drug-resistant cells suppresses Hippo signaling, promoting YAP activation and nuclear translocation. EGF stimulation further amplifies this effect by increasing the phosphorylation of EGFR and downstream proteins, including YAP, LATS1, and MOB1. Knockdown of PD-L1 or inhibition of YAP with Verteporfin reverses this activation, reactivating Hippo signaling and inhibiting YAP transcriptional activity. These findings provide potential therapeutic targets for overcoming drug resistance.

PD-L1 enhances Wnt/β-catenin signaling through β-catenin phosphorylation and nuclear translocation in osimertinib resistance

In the OR group, EGFR mutations activate the Wnt signaling pathway, resulting in the phosphorylation and nuclear translocation of Ser552-β-catenin, which subsequently increases PD-L1 expression (**Figure 4C**). Importantly, inhibiting PD-L1 expression reduces Wnt-induced phosphorylation of β-catenin at Ser552 while enhancing the activity of the non-phosphorylated form of β-catenin. PD-L1 upregulation enhances Wnt/β-catenin signaling by increasing β-catenin phosphorylation and stabilization, thus contributing to drug resistance.

As expected, in the OR group, TGF stimulation led to increased phosphorylation of p-EGFR at Y1068, which in turn enhanced the transcriptional activity of β-catenin (both total and active forms) and activated the downstream Wnt/β-catenin signaling pathway. In both resistant cell groups, treatment with XAV939 and IWR-1-endo inhibitor significantly reduced β-catenin stability and S552 phosphorylation. However, no significant change in Ser552 phosphorylation was observed in the Sh-PD-L1-OR group. These findings suggest that Wnt/β-catenin signaling pathway transduction is positively correlated with PD-L1 expression. High PD-L1 expression enhances the activity of YAP and β-catenin by upregulating their transcriptional activity, total expression, and nuclear translocation, while reduced PD-L1 expression impedes this pathway.

In the OR group, YAP inhibition resulted in a decrease in phosphorylated YAP (Ser127) and total YAP expression, while the expression of LATS1 was reduced, and the phosphorylation of LATS1 (Ser909) remained unchanged (**Figure 4D**). Wnt signaling was upregulated, with increased levels of β-catenin and phosphorylated β-catenin (Ser552). In the Sh-PD-L1-OR group, YAP inhibition further decreased both YAP and phospho-YAP (Ser127) levels. Wnt silencing significantly reduced both β-catenin and phosphorylated β-catenin levels. In summary, the experiment demonstrates that both YAP inhibition and Wnt silencing affect the regulation of YAP, LATS1, and β-catenin signaling pathways, with PD-L1 playing a crucial role in resistance-induced interactions within this pathway.

PD-L1 mediates the interaction between YAP and β-catenin in the drug resistance process

Endogenous immunoprecipitation (IP) results demonstrated that β-catenin co-precipitated with endogenous YAP, indicating a stable protein-protein interaction between the two within the cell (**Figure 5A**). Following the induction of resistance, CO-IP analysis revealed a significant enhancement in the interaction between β-catenin and YAP in the OR group, with the formation of the YAP/TAZ complex (**Figure 5B**). In contrast, Sh-PD-L1-OR cells exhibited a marked reduction in the resistance-induced interaction between β-catenin and YAP.

GSK3β is a critical regulator involved in multiple cell signaling pathways, including the Hippo and Wnt/β-catenin pathways, both of which play essential roles in cell growth, differentiation, and tumorigenesis [33]. Modulation of GSK3β activity has been implicated in resistance mechanisms in non-small cell lung cancer (NSCLC), particularly in the context of osimertinib treatment [34]. In the OR group, PD-L1 upregulation inhibits GSK3β activation, as indicated by increased p-GSK3β (Ser9) and decreased p-GSK3β (Tyr216) levels (**Figure 5C**). In contrast, in the Sh-PD-L1-OR group, PD-L1 knockdown leads to increased phosphorylation of GSK3β at Tyr216, indicating enhanced activation of GSK3β, while phosphorylation at Ser9 decreased, suggesting reactivation of GSK3β. These findings suggest that PD-L1 upregulation inhibits GSK3β activity in resistant cells, while PD-L1 knockdown restores its activation.

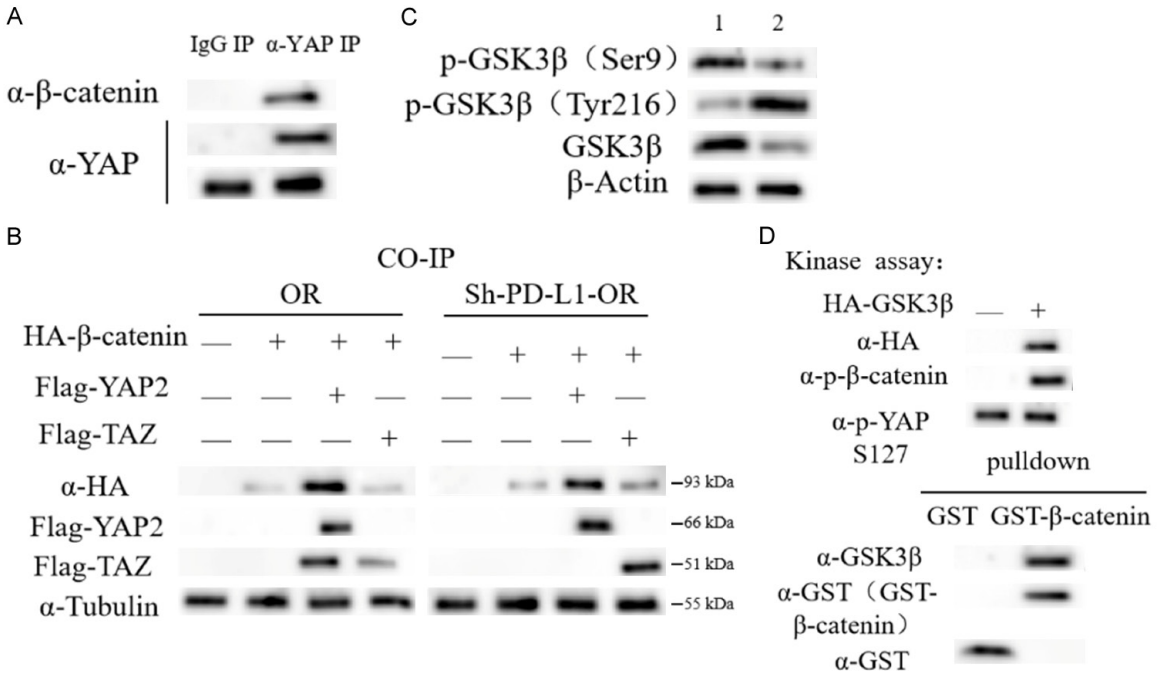

Figure 5. PD-L1 mediates the interaction between YAP and β-Catenin in drug resistance process. A. Co-precipitation of endogenous YAP and β-catenin. B. CO-IP detection of the interaction between YAP and β-catenin proteins after drug resistance. C. Expression of GSK3β protein (1 and 2 represent OR and Sh-PD-L1-OR groups, respectively). D. Phosphorylation and pulldown experiments after overexpression of β-catenin.

Furthermore, overexpression of GSK3β significantly increased the phosphorylation of YAP (S127) and β-catenin (**Figure 5D**). Pulldown assays demonstrated that the interaction between GSK3β and β-catenin was strengthened with the increased phosphorylation of YAP at Ser127.

Anlotinib resensitizes osimertinib-resistant cells by inhibiting the YAP/β-catenin pathway and enhances antitumor activity

After 72 h of treatment, osimertinib-resistant cells with both high and low PD-L1 expression exhibited a more compact, epithelial-like morphology upon anlotinib treatment. The Sh-PD-L1-OR group showed a more marked reduction in mesenchymal-like features, indicating partial reversal of EMT (**Figure 6A** and **6B**). MTT assay results (**Figure 6C**) confirmed that anlotinib significantly decreased the viability of these cells, with a more pronounced effect in the Sh-PD-L1-OR group ($P < 0.001$). Anlotinib also notably reduced cell migration in the OR group ($P < 0.05$, **Figure 6E**), and when combined with PD-L1 knockdown, this effect was further enhanced ($P < 0.01$, **Figure 6D**). Additionally, anlotinib treatment reduced colony formation in OR cells, and PD-L1 knockdown further diminished invasion ($P < 0.01$, **Figure 6F**). Anlotinib treatment also significantly induced apoptosis in the OR cells, with the Sh-PD-L1-OR group showing a greater increase in apoptotic cells ($P < 0.05$, **Figure 6G**). These findings suggest that anlotinib effectively inhibits migration, invasion, and resistance to apoptosis in osimertinib-resistant cells. The effect was further potentiated by low PD-L1 expression, mimicking clinical conditions with PD-L1 low-expression tumors.

Anlotinib treatment decreased the expression of p-EGFR and PD-L1 in OR cells, with the Sh-PD-L1-OR group showing more substantial reductions (**Figure 6H**). Notably, anlotinib treatment led to a decrease in YAP dephosphorylation and phosphorylation levels in the OR group (**Figure 6I**). While the downstream protein MOB1 showed no change in expression, its phosphorylation increased, and the expression of LAST protein decreased, with its phosphorylation rising. Additionally, the phosphorylation level of β-catenin (ps552) increased in the OR group, indicating enhanced Wnt signaling, while

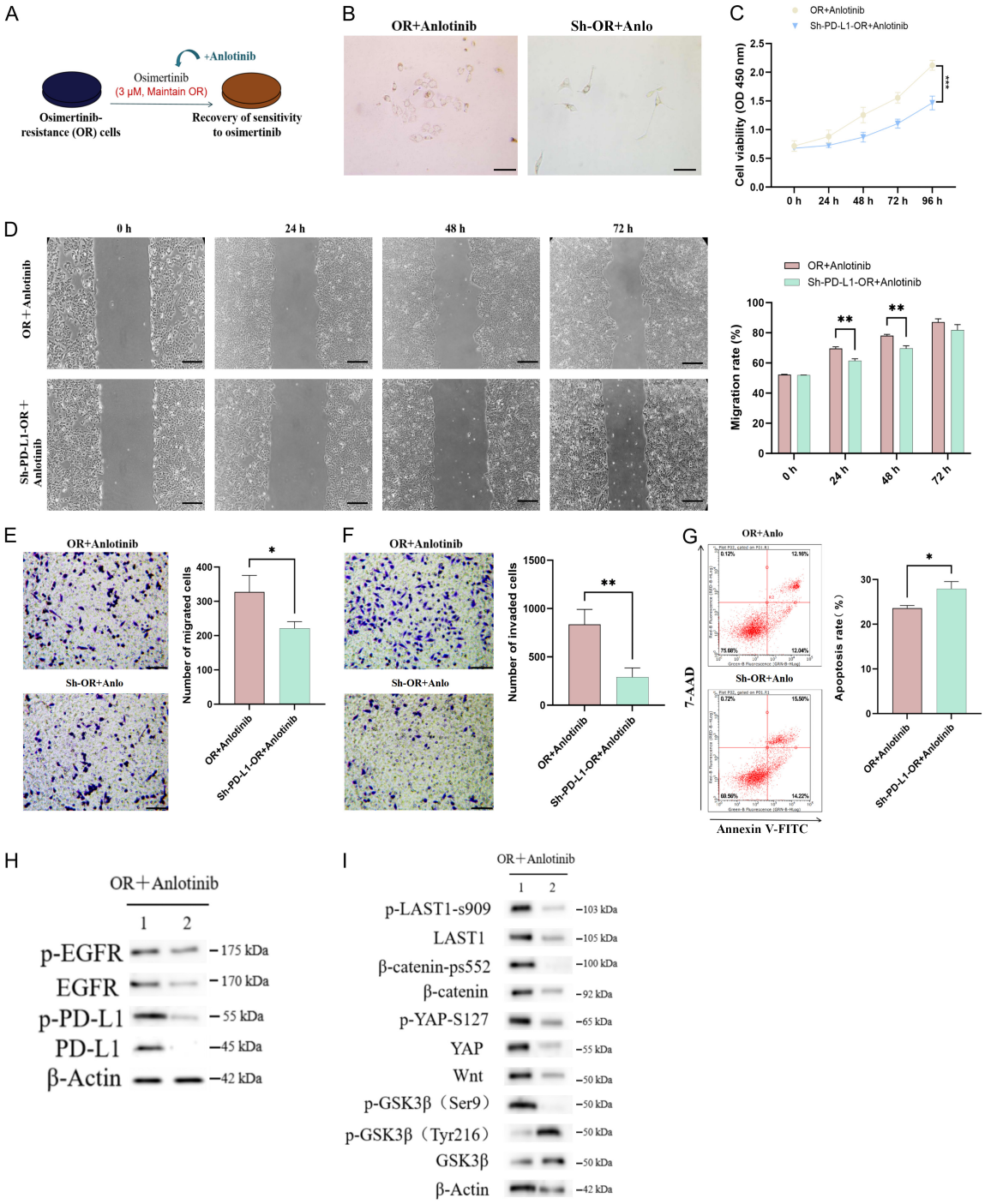

Figure 6. Anlotinib restores osimertinib sensitivity in resistant cells by inhibiting the YAP/β-catenin axis, synergistically enhancing antitumor effects in vitro. A. Osimertinib-resistant cells with high and low PD-L1 expression were treated with 3 μM osimertinib (maintaining resistance), 1 μM anlotinib (treatment), or both for 72 h. B. Cell morphology was observed under a microscope (Scale Bar: 100 μm; original magnification, ×200). C. Cell viability was measured using the MTT assay. D, E. Migration rates and cell migration capacity at different time points were assessed using scratch and transwell assays (Scale Bar: 100 μm; original magnification, ×200). F. Colony formation assays were conducted to evaluate cell invasion ability (Scale Bar: 100 μm; original magnification, ×200). G. Apoptosis was detected by Annexin V-FITC/7-AAD. H and I. Western blotting was performed to assess the expression of p-EGFR, EGFR, p-PD-L1, PD-L1, and proteins related to the YAP and Wnt signaling pathways (1 and 2 represent the OR group and the Sh-PD-L1-OR group respectively). *$P < 0.05$, **$P < 0.01$, ***$P < 0.001$.

its phosphorylation was significantly reduced in the Sh-PD-L1-OR group. β-catenin expression was higher in the OR group compared to the Sh-PD-L1-OR group. Activation of GSK3β was linked to phosphorylation at Ser9 and Tyr216, and after anlotinib treatment, GSK3β activation in the OR group was significantly increased, with reduced p-GSK3β (Ser9) and increased p-GSK3β (Tyr216) levels. In Sh-PD-L1-OR cells, anlotinib treatment further decreased β-catenin expression, likely due to increased GSK3β expression (**Figure 6I**). Furthermore, anlotinib significantly promoted the phosphorylation of YAP (Ser127) in Sh-PD-L1-OR cells, thereby activating the Hippo pathway.

These results suggest that anlotinib can restore osimertinib sensitivity in NSCLC by inhibiting Wnt signaling and activating the Hippo pathway. Moreover, low PD-L1 expression may enhance anlotinib's therapeutic efficacy in overcoming resistance.

Synergistic antitumor effect of anlotinib combination therapy with PD-L1 inhibition

The experimental timeline outlines the in vivo treatment protocol, where mice were treated with Anlotinib or PBS for 21 days, with tumor growth monitored at multiple time points (**Figure 7A**). After 21 days of treatment, tumors in the Anlotinib-treated group were significantly smaller than those in the OR group (**Figure 7B**, **7C**). Specifically, the Sh-PD-L1-OR group demonstrated slower tumor growth and weight increase from Day 5 to Day 21, compared to the OR group (both $P < 0.001$, **Figure 7D**, **7E**). Additionally, a significant reduction in tumor weight was observed in the Sh-PD-L1-OR group ($P < 0.01$, **Figure 7B**).

Tumor sections stained with HE revealed morphological changes, indicating reduced tumor cell proliferation and increased cell death in the combination treatment group compared to single treatments (**Figure 7F**). IHC for EGFR and PD-L1 confirmed significant reductions in the expression of these proteins in the tumors, suggesting effective inhibition of both EGFR and PD-L1 pathways. IHC analysis of YAP expression further demonstrated that Anlotinib treatment significantly downregulated YAP in tumor tissues (**Figure 7G**). Similarly, β-catenin expression was markedly decreased in tumors treated with Anlotinib. In line with in vitro results, the combined treatment with PD-L1 inhibition interfered with the YAP/β-catenin axis, further inhibiting tumor growth.

Discussion

Previous studies have demonstrated that EGFR activating mutations in HCC827 cells are closely linked to the upregulation of PD-L1 expression, and that EGFR-TKIs can significantly reduce PD-L1 expressio [32]. In our previous research, we found that among patients with EGFR mutations, 54% had exon 19 deletions, while 46% exhibited the exon 21 L858R mutation [12]. 150 patients were assessed for PD-L1 expression, of which 89 (59.33%) were negative (TPS < 1%), 42 (28%) had weak expression (1-49%), and 19 (12.66%) had strong expression (≥ 50%). Of these, 65.33% were treated with osimertinib, and 34.66% received aumolertinib. Based on these findings, we selected the HCC827 cell line, which exhibits high PD-L1 expression, as the control group and performed PD-L1 knockdown. Subsequent drug resistance studies revealed that the downregulation of PD-L1 significantly reduced both PD-L1 and EGFR expression, thereby enhancing the sensitivity of osimertinib-resistant cells to treatment. We observed morphological changes consistent with EMT in the osimertinib-resistant cells. Resistance-related markers, such as N-cadherin and Vimentin, were significantly upregulated in both the OR and Sh-PD-L1-OR groups, while E-cadherin expression was reduced. Notably, PD-L1 knockdown in the Sh-PD-L1-OR group led to a decrease in N-cadherin and Vimentin expression compared to the OR group, suggesting that PD-L1 plays a critical role in regulating the EMT process associated with the acquisition of resistance. These results are consistent with previous studies, which indicate that PD-L1 contributes to resistance by promoting EMT and enhancing cell migration and invasion [29].

YAP, a downstream target of the Hippo signaling pathway, is overexpressed in various cancers, including lung cancer, breast cancer, colorectal cancer, and oral cancer, with YAP/TAZ being recognized as oncogenic factors [35-38]. Increased YAP expression is observed in 66.3% of NSCLC samples, correlating significantly with staging and lymph node metastasis [35, 39]. To explore the role of PD-L1 in regulat-

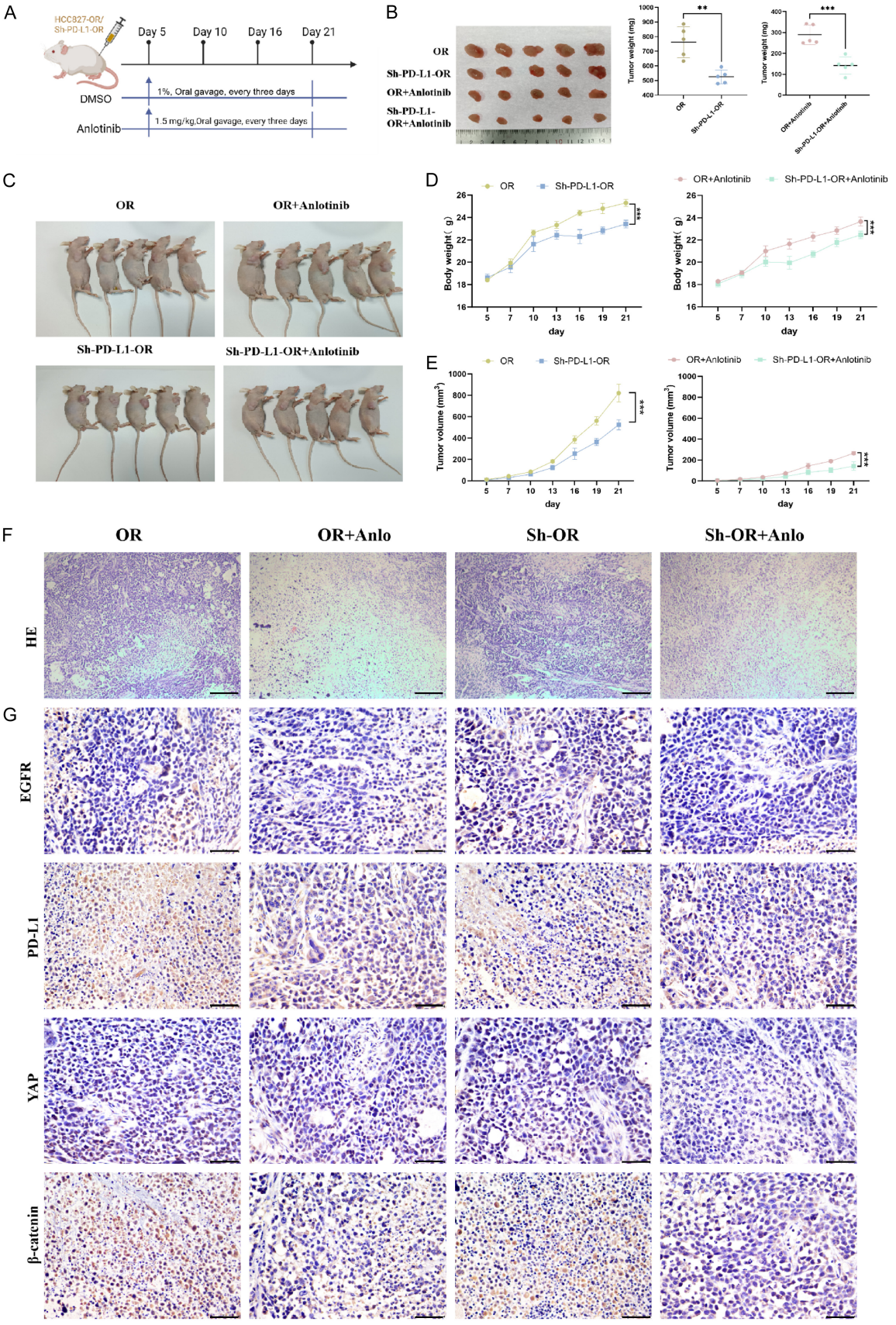
A
HCC827-OR/
Sh-PD-L1-OR
Day 5
Day 10
Day 16
Day 21
DMSO
1%, Oral gavage, every three days
Anlotinib
1.5 mg/kg,Oral gavage, every three days
B
OR
Sh-PD-L1-OR
OR+Anlotinib
Sh-PD-L1-OR+Anlotinib
Tumor weight (mg)
C
OR
OR+Anlotinib
Sh-PD-L1-OR
Sh-PD-L1-OR+Anlotinib
D
Body weight(g)
day
E
Tumor volume (mm3)
day
F
OR
OR+Anlo
Sh-OR
Sh-OR+Anlo
HE
G
EGFR
PD-L1
YAP
β-catenin

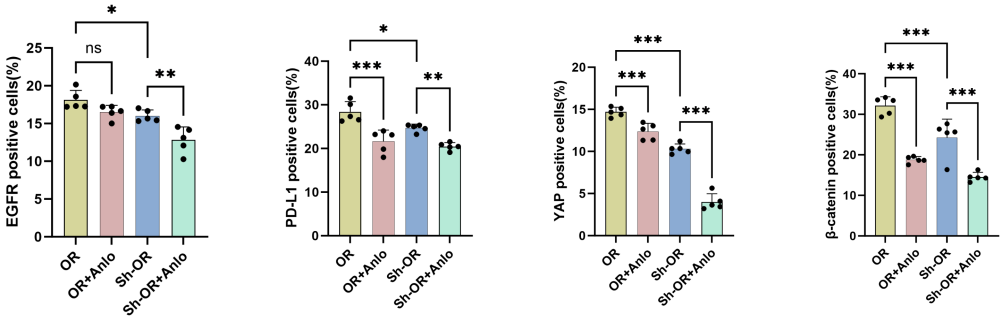

Figure 7. Antitumor effect of combined anlotinib treatment in PD-L1 high and low expression mouse models. A. Schematic diagram of the vivo experimental procedure. B. Macroscopic appearance of tumors after 21 days of treatment (n = 5). C. Body weight measurements were taken starting from Day 5, with monitoring every three days. The body weight growth curve over the 21-day period is shown. D. On Day 22, mice were euthanized, and tumors were harvested. The tumor weights were recorded following 21 days of treatment (n = 5). E. Tumor volume was measured starting on Day 5, and tumor volume growth curves were plotted over time, with measurements taken every three days. F, G. Hematoxylin and eosin (H&E) staining alongside immunohistochemical (IHC) analysis of EGFR, PD-L1, YAP, and β-catenin expression in tumor tissues from different treatment groups (Scale Bar: 50 μm; original magnification, ×200). G. Includes a semi-quantitative analysis of the positive cell percentages for each marker, demonstrating the relative expression levels across groups. s.c., subcutaneous injection. $*P < 0.05$, $**P < 0.01$, $***P < 0.001$.

ing the YAP and Hippo pathways, we examined their interplay in the context of PD-L1 overexpression. The Hippo pathway involves MST1/2 kinases, LATS1/2 kinases, and adaptor proteins Sav and MOB1 [40]. When activated, MST1/2 phosphorylates LATS1/2 and MOB1, forming the LATS/MOB1 complex, which in turn phosphorylates and inactivates YAP [41]. In the OR group, PD-L1 upregulation enhanced YAP phosphorylation and nuclear translocation, thereby increasing YAP transcriptional activity. Concurrently, expression of Hippo pathway proteins LATS1 and MOB1 was elevated, but their phosphorylation levels were reduced, indicating inhibition of LATS1/2 complex activity. This inhibition activated YAP signaling, promoting its nuclear translocation and enhancing transcriptional function. PD-L1 knockdown in the Sh-PD-L1-OR group reversed these effects, evidenced by increased phosphorylation of LATS1 and MOB1, resulting in reduced YAP activation.

Moreover, EGFR TKI treatment has been shown to increase nuclear β-catenin (both total and active forms) and reduce phosphorylated β-catenin (inactive form) [33]. In resistance, increased phosphorylated β-catenin suggests a decrease in its stable form. Additionally, Wnt signaling has been reported to trans-activate EGFR in other cancers, with a significant positive correlation observed between activated EGFR mutations and nuclear β-catenin accumulation in primary NSCLC. In the OR group, EGFR mutations activated Wnt signaling, resulting in β-catenin phosphorylation at Ser552 and its nuclear translocation, which in turn enhanced PD-L1 expression. Inhibition of PD-L1 expression significantly reduced β-catenin phosphorylation at Ser552, while enhancing non-phosphorylated β-catenin activity. These findings suggest that PD-L1 upregulation stabilizes β-catenin, promoting its phosphorylation and activating the Wnt/β-catenin signaling pathway, thereby contributing to resistance. Furthermore, TGF-induced phosphorylation of EGFR at Y1068 augmented β-catenin transcriptional activity, further activating downstream Wnt signaling. This was confirmed using XAV-939 and IWR-1-endo inhibitors, which reduced β-catenin stability and phosphorylation at Ser552 in both resistant cell groups.

The role of EGFR-induced PD-L1 upregulation in regulating YAP and Hippo signaling pathways after drug resistance remains unclear. Previous studies have shown that YAP is a target of the Wnt signaling pathway, with GSK3β acting as a key regulator linking the Hippo and Wnt/β-catenin pathways [42, 43]. To explore whether EGFR-induced PD-L1 upregulation regulates YAP through GSK3β and Wnt pathways, we used XAV-939 to reverse the effects of PD-L1 upregulation on YAP, LATS1, and MOB1. In the low PD-L1 expression group, XAV-939 signifi-

cantly decreased YAP and LATS expression, suggesting that PD-L1 regulates YAP through GSK3β and Wnt pathways. The YAP inhibitor Vitipofen also reversed PD-L1-induced Wnt and β-catenin upregulation, with reduced β-catenin and Wnt levels in the low PD-L1 expression group. These results indicate that EGFR-induced PD-L1 upregulation regulates YAP and its downstream targets by modulating GSK3β and Wnt signaling, contributing to resistance.

Anlotinib, a multi-target tyrosine kinase inhibitor, has demonstrated efficacy in NSCLC by inhibiting angiogenesis through targeting c-MET, MYC, and AXL. Recent studies have shown that anlotinib can reverse osimertinib resistance in EGFR T790M-mutant NSCLC cells by inhibiting the c-MET/MYC/AXL axis, enhancing osimertinib efficacy [29]. Clinical trials have indicated that combining anlotinib with osimertinib provides significant therapeutic benefits with a manageable safety profile, making it a promising option to overcome resistance in NSCLC [44-46]. Moreover, the combination of anlotinib and PD-L1 inhibitors has shown potential by enhancing the immune response and inhibiting angiogenesis [47-50]. Notably, low-dose anlotinib combined with PD-1 blockade effectively inhibits tumor growth and enhances immune cell infiltration with fewer side effects compared to high doses [51]. Previous studies have demonstrated that anlotinib combined with anti-PD-1/PD-L1 therapy shows promising efficacy and tolerability in EGFR-TKI-resistant NSCLC patients, with encouraging response rates and manageable safety profiles, highlighting its potential as a therapeutic option for overcoming resistance in these patients [52]. However, the underlying mechanisms remain to be fully elucidated.

This study found that anlotinib combined with osimertinib and PD-L1 inhibition restored the sensitivity of drug-resistant NSCLC cells to osimertinib. Anlotinib treatment reversed mesenchymal-like morphology, reduced cell viability, migration, and invasion, and increased apoptosis, with greater effects observed in the Sh-PD-L1-OR group. Mechanistically, anlotinib inhibited the YAP/β-catenin signaling axis, decreased YAP phosphorylation and β-catenin stability, and activated the Hippo pathway, as evidenced by increased GSK3β phosphorylation. In vivo, the combination therapy reduced tumor growth and weight, with decreased expression of EGFR, PD-L1, YAP, and β-catenin. These results highlight the therapeutic potential of combining anlotinib with osimertinib and PD-L1 inhibition to overcome drug resistance in NSCLC. In summary, our findings suggest that EGFR-induced PD-L1 upregulation not only modulates tumor cell-intrinsic resistance mechanisms but also interacts with anlotinib's therapeutic action, highlighting a potential synergistic effect. Beyond its established anti-angiogenic effects, anlotinib has been shown to modulate the tumor immune microenvironment, promoting immune cell infiltration and reducing PD-L1 expression, thus reprogramming immunosuppressive niches [53]. This immune-modulatory effect is likely synergistic with its inhibition of the YAP/β-catenin axis, a key resistance pathway in NSCLC. Our data indicate that anlotinib promotes GSK3β activation and stabilizes the Hippo pathway, leading to the inhibition of YAP activity and reduced β-catenin stability, which together counteract the resistance phenotype [54-56]. These findings suggest that combining anlotinib with EGFR inhibitors, such as osimertinib, and PD-L1 inhibitors could provide a multi-pronged approach to overcoming resistance in NSCLC. Future studies should explore the clinical validation of these mechanisms and investigate potential biomarkers for patient-specific treatment strategies.

The relationship between PD-L1 and EGFR expression in EGFR-mutant NSCLC is complex and context-dependent. In experimental models of EGFR-TKI resistance, EGFR signaling activation often leads to PD-L1 upregulation, suggesting a positive correlation between these two molecules. However, clinical data, such as those from the TCGA database, reveal a negative correlation, indicating that the interaction between PD-L1 and EGFR expression may be influenced by factors like tumor heterogeneity or immune evasion mechanisms. These discrepancies highlight the need for further clinical validation, as our study lacks patient-derived models and clinical data, which limits the direct applicability of our findings. While the Co-IP and pharmacological inhibition experiments suggest an interaction and functional correlation between PD-L1 and GSK3β/Wnt/Hippo signaling, definitive proof of direct regulation of GSK3β activity by PD-L1 would require more direct assays, such as in vitro kinase assays. We acknowledge this limitation and

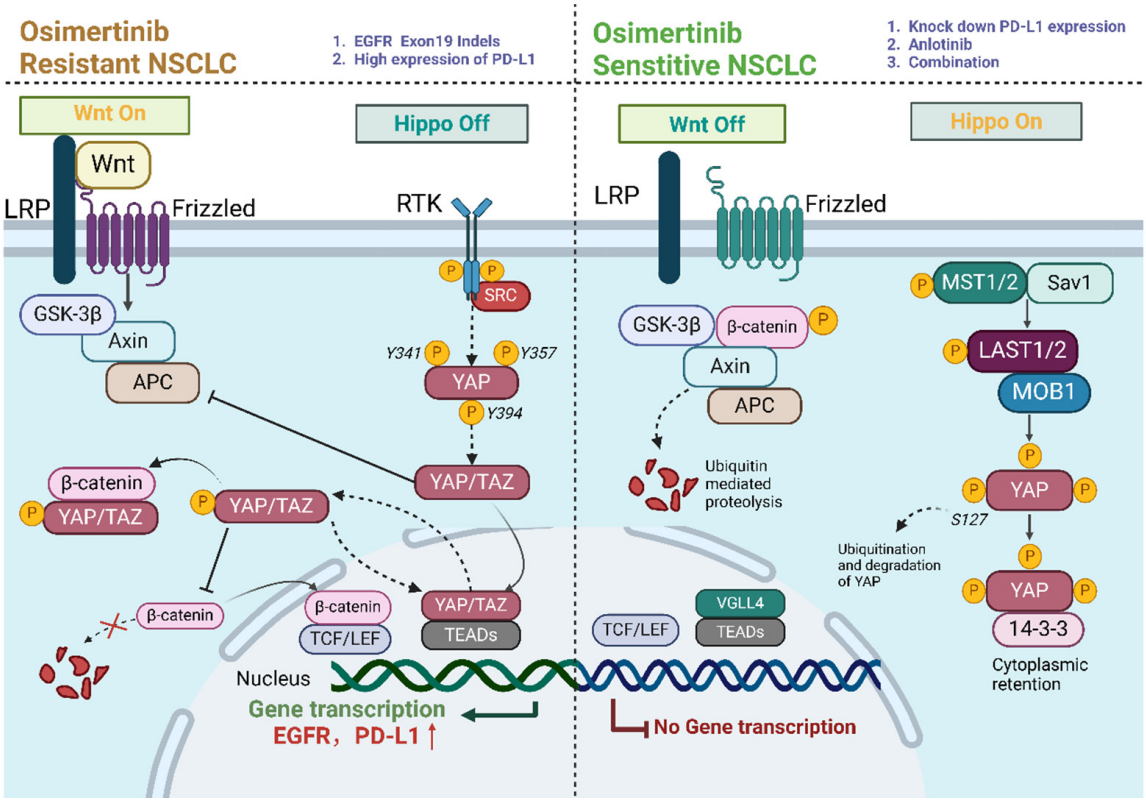

Figure 8. Anlotinib overcomes EGFR Mutation-Induced resistance in NSCLC by targeting PD-L1 and modulating Wnt/β-catenin and Hippo/YAP pathways.

suggest that future research, including the use of PD-L1 mutants and kinase assays, will be necessary to establish the direct regulatory mechanism. Future research should focus on validating these mechanisms in clinical settings and exploring biomarkers that could help in patient stratification for more personalized treatments.

Conclusion

This study underscores the pivotal role of PD-L1 in mediating osimertinib resistance in EGFR-mutant NSCLC. EGFR-induced PD-L1 upregulation modulates both the Hippo/YAP and Wnt/β-catenin pathways, promoting resistance (**Figure 8**). PD-L1 upregulation inhibits the Hippo pathway, leading to increased YAP nuclear translocation and activity, while also enhancing β-catenin phosphorylation and nuclear accumulation, thereby activating the Wnt/β-catenin pathway. Knockdown of PD-L1 disrupts these signaling cascades, reactivating the Hippo pathway, reducing YAP activity, and inhibiting β-catenin phosphorylation and translocation. This results in significantly decreased cell viability, migration, invasion, and increased apoptosis, indicating that PD-L1 inhibition can delay or reverse resistance. Treatment with anlotinib, a multikinase inhibitor, resensitized resistant cells by targeting both YAP and β-catenin signaling, reducing cell aggressiveness and enhancing apoptosis. Combined with PD-L1 knockdown, anlotinib further amplified these effects, suggesting a synergistic action in overcoming drug resistance. These findings establish PD-L1 as a key modulator of EGFR-driven resistance through the Hippo/YAP and Wnt/β-catenin pathways.

Acknowledgements

This work was supported by the National Natural Science Foundation of China (Grant No. 82473254), Clinical Research Pioneering Program of Shandong First Medical University & Shandong Academy of Medical Sciences (607D25022), Wu Jieping Medical Foundation (320.6750.2023-16-6,320.6750.2025-20-12), and China Zhongguancun Precision Medicine Science and Technology Foundation (GXZDH72).

Disclosure of conflict of interest

The authors declare that the research was conducted in the absence of any commercial or financial relationships that could be construed as a potential conflict of interest.

Abbreviations

NSCLC, non-small cell lung cancer; EGFR, epidermal growth factor receptor; TKI, tyrosine kinase inhibitor; OR, osimertinib-resistant; Sh-PD-L1, stable PD-L1 knockdown; PD-L1, programmed death-ligand 1; PD-1, programmed cell death protein-1; ICI, immune checkpoint inhibitor; EMT, epithelial-mesenchymal transition; YAP, Yes-associated protein; Wnt/β-catenin, Wingless/β-catenin pathway; GSK3β, glycogen synthase kinase-3β; EGF, epidermal growth factor.

Address correspondence to: Jinming Yu and Hui Zhu, Shandong University Cancer Center, Jinan 250-117, Shandong, China; Department of Radiation Oncology, Shandong Cancer Hospital and Institute, Shandong First Medical University and Shandong Academy of Medical Sciences, Jinan 250117, Shandong, China. E-mail: sdyujinming@163.com (JMY); drzhuh@126.com (HZ)

References

[1] Zhang A, Yang F, Gao L, Shi X and Yang J. Research progress on radiotherapy combined with immunotherapy for associated pneumonitis during treatment of non-small cell lung cancer. Cancer Manag Res 2022; 14: 2469-2483.

[2] Luo J, Cheng K, Ji X, Gao C, Zhu R, Chen J, Xue W, Huang Q and Xu Q. Anlotinib enhanced CD8+ T cell infiltration via induction of CCL5 improves the efficacy of PD-1/PD-L1 blockade therapy in lung cancer. Cancer Lett 2024; 591: 216892.

[3] Ettinger DS, Wood DE, Aisner DL, Akerley W, Bauman JR, Bharat A, Bruno DS, Chang JY, Chirieac LR, DeCamp M, Dilling TJ, Dowell J, Durm GA, Gettinger S, Grotz TE, Gubens MA, Hegde A, Lackner RP, Lanuti M, Lin J, Loo BW, Lovly CM, Maldonado F, Massarelli E, Morgensztern D, Ng T, Otterson GA, Patel SP, Patil T, Polanco PM, Riely GJ, Riess J, Schild SE, Shapiro TA, Singh AP, Stevenson J, Tam A, Tanvetyanon T, Yanagawa J, Yang SC, Yau E, Gregory KM and Hughes M. NCCN Guidelines® insights: non-small cell lung cancer, version 2.2023. J Natl Compr Canc Netw 2023; 21: 340-350.

[4] Siegel RL, Miller KD and Jemal A. Cancer statistics, 2020. CA Cancer J Clin 2020; 70: 7-30.

[5] Remon J, Steuer CE, Ramalingam SS and Felip E. Osimertinib and other third-generation EGFR TKI in EGFR-mutant NSCLC patients. Ann Oncol 2018; 29: i20-i27.

[6] Soria JC, Ohe Y, Vansteenkiste J, Reungwetwattana T, Chewaskulyong B, Lee KH, Dechaphunkul A, Imamura F, Nogami N, Kurata T, Okamoto I, Zhou C, Cho BC, Cheng Y, Cho EK, Voon PJ, Planchard D, Su WC, Gray JE, Lee SM, Hodge R, Marotti M, Rukazenkov Y and Ramalingam SS; FLAURA Investigators. Osimertinib in untreated EGFR-mutated advanced non-small-cell lung cancer. N Engl J Med 2018; 378: 113-125.

[7] Alsaab HO. Pathological role of long non-coding (lnc) RNA in the regulation of Wnt/β-catenin signaling pathway during epithelial-mesenchymal transition (EMT). Pathol Res Pract 2023; 248: 154566.

[8] Haratani K, Hayashi H, Tanaka T, Kaneda H, Togashi Y, Sakai K, Hayashi K, Tomida S, Chiba Y, Yonesaka K, Nonagase Y, Takahama T, Tanizaki J, Tanaka K, Yoshida T, Tanimura K, Takeda M, Yoshioka H, Ishida T, Mitsudomi T, Nishio K and Nakagawa K. Tumor immune microenvironment and nivolumab efficacy in EGFR mutation-positive non-small-cell lung cancer based on T790M status after disease progression during EGFR-TKI treatment. Ann Oncol 2017; 28: 1532-1539.

[9] Cho JH, Zhou W, Choi YL, Sun JM, Choi H, Kim TE, Dolled-Filhart M, Emancipator K, Rutkowski MA and Kim J. Retrospective molecular epidemiology study of PD-L1 expression in patients with EGFR-mutant non-small cell lung cancer. Cancer Res Treat 2018; 50: 95-102.

[10] Nicolazzo C, Raimondi C, Mancini M, Caponnetto S, Gradilone A, Gandini O, Mastromartino M, Del Bene G, Prete A, Longo F, Cortesi E and Gazzaniga P. Monitoring PD-L1 positive circulating tumor cells in non-small cell lung cancer patients treated with the PD-1 inhibitor Nivolumab. Sci Rep 2016; 6: 31726.

[11] Sheng J, Fang W, Yu J, Chen N, Zhan J, Ma Y, Yang Y, Huang Y, Zhao H and Zhang L. Expression of programmed death ligand-1 on tumor cells varies pre and post chemotherapy in non-small cell lung cancer. Sci Rep 2016; 6: 20090.

[12] Niu J, Jing X, Xu Q, Liu H, Tian Y, Yang Z, Zhu H and Sun Y. Strong PD-L1 affect clinical outcomes in advanced NSCLC treated with third-generation EGFR-TKIs. Future Oncol 2024; 20: 2481-2490.

[13] Tsutsumi S, Saeki H, Nakashima Y, Ito S, Oki E, Morita M, Oda Y, Okano S and Maehara Y. Programmed death-ligand 1 expression at tumor invasive front is associated with epithelial-mesenchymal transition and poor prognosis in esophageal squamous cell carcinoma. Cancer Sci 2017; 108: 1119-1127.

[14] Jia Y, Zhao S, Jiang T, Li X, Zhao C, Liu Y, Han R, Qiao M, Liu S, Su C, Ren S and Zhou C. Impact of EGFR-TKIs combined with PD-L1 antibody on the lung tissue of EGFR-driven tumor-bearing mice. Lung Cancer 2019; 137: 85-93.
[15] Jia Y, Li X, Jiang T, Zhao S, Zhao C, Zhang L, Liu X, Shi J, Qiao M, Luo J, Liu S, Han R, Su C, Ren S and Zhou C. EGFR-targeted therapy alters the tumor microenvironment in EGFR-driven lung tumors: implications for combination therapies. Int J Cancer 2019; 145: 1432-1444.
[16] Harris SJ, Brown J, Lopez J and Yap TA. Immuno-oncology combinations: raising the tail of the survival curve. Cancer Biol Med 2016; 13: 171-193.
[17] Puzanov I, Diab A, Abdallah K, Bingham CO 3rd, Brogdon C, Dadu R, Hamad L, Kim S, Lacouture ME, LeBoeuf NR, Lenihan D, Onofrei C, Shannon V, Sharma R, Silk AW, Skondra D, Suarez-Almazor ME, Wang Y, Wiley K, Kaufman HL and Ernstoff MS; Society for Immunotherapy of Cancer Toxicity Management Working Group. Managing toxicities associated with immune checkpoint inhibitors: consensus recommendations from the Society for Immunotherapy of Cancer (SITC) toxicity management working group. J Immunother Cancer 2017; 5: 95.
[18] To KKW, Fong W and Cho WCS. Immunotherapy in treating EGFR-mutant lung cancer: current challenges and new strategies. Front Oncol 2021; 11: 635007.
[19] Shen G, Zheng F, Ren D, Du F, Dong Q, Wang Z, Zhao F, Ahmad R and Zhao J. Anlotinib: a novel multi-targeting tyrosine kinase inhibitor in clinical development. J Hematol Oncol 2018; 11: 120.
[20] Sun Y, Niu W, Du F, Du C, Li S, Wang J, Li L, Wang F, Hao Y, Li C and Chi Y. Safety, pharmacokinetics, and antitumor properties of anlotinib, an oral multi-target tyrosine kinase inhibitor, in patients with advanced refractory solid tumors. J Hematol Oncol 2016; 9: 105.
[21] Syed YY. Anlotinib: first global approval. Drugs 2018; 78: 1057-1062.
[22] Zhang W, Yang H, Kong T and Han B. 355P anlotinib plus standard chemotherapy as first-line treatment in extensive-stage small cell lung cancer patients. Ann Oncol 2022; 33: S1580.
[23] Liu C, Liao J, Wu X, Zhao X, Sun S, Wang H, Hu Z, Zhang Y, Yu H and Wang J. A phase II study of anlotinib combined with etoposide and platinum-based regimens in the first-line treatment of extensive-stage small cell lung cancer. Thorac Cancer 2022; 13: 1463-1470.
[24] Huang M, Liu Y, Yu M, Li Y, Zhang Y, Zhu J, Li L and Lu Y. A phase I study of the tyrosine kinase inhibitor anlotinib combined with platinum/pemetrexed-based chemotherapy in untreated nonsquamous non-small-cell lung cancer. Invest New Drugs 2022; 40: 308-313.
[25] Garber K. Promising early results for immunotherapy-antiangiogenesis combination. J Natl Cancer Inst 2014; 106: dju392.
[26] Chu T, Zhong R, Zhong H, Zhang B, Zhang W, Shi C, Qian J, Zhang Y, Chang Q, Zhang X, Dong Y, Teng J, Gao Z, Qiang H, Nie W, Zhao Y, Han Y, Chen Y and Han B. Phase 1b study of sintilimab plus anlotinib as first-line therapy in patients with advanced NSCLC. J Thorac Oncol 2021; 16: 643-652.
[27] Zhou W, Gao Y, Tong Y, Wu Q, Zhou Y and Li Y. Anlotinib enhances the antitumor activity of radiofrequency ablation on lung squamous cell carcinoma. Pharmacol Res 2021; 164: 105392.
[28] Li T, Qian Y, Zhang C, Uchino J, Provencio M, Wang Y, Shi X, Zhang Y and Zhang X. Anlotinib combined with gefitinib can significantly improve the proliferation of epidermal growth factor receptor-mutant advanced non-small cell lung cancer in vitro and in vivo. Transl Lung Cancer Res 2021; 10: 1873-1888.
[29] Lei T, Xu T, Zhang N, Zou X, Kong Z, Wei C and Wang Z. Anlotinib combined with osimertinib reverses acquired osimertinib resistance in NSCLC by targeting the c-MET/MYC/AXL axis. Pharmacol Res 2023; 188: 106668.
[30] Lee BS, Park DI, Lee DH, Lee JE, Yeo MK, Park YH, Lim DS, Choi W, Lee DH, Yoo G, Kim HB, Kang D, Moon JY, Jung SS, Kim JO, Cho SY, Park HS and Chung C. Hippo effector YAP directly regulates the expression of PD-L1 transcripts in EGFR-TKI-resistant lung adenocarcinoma. Biochem Biophys Res Commun 2017; 491: 493-499.
[31] Tung JN, Lin PL, Wang YC, Wu DW, Chen CY and Lee H. PD-L1 confers resistance to EGFR mutation-independent tyrosine kinase inhibitors in non-small cell lung cancer via upregulation of YAP1 expression. Oncotarget 2018; 9: 4637-4646.
[32] Chen N, Fang W, Zhan J, Hong S, Tang Y, Kang S, Zhang Y, He X, Zhou T, Qin T, Huang Y, Yi X and Zhang L. Upregulation of PD-L1 by EGFR activation mediates the immune escape in EGFR-driven NSCLC: implication for optional immune targeted therapy for NSCLC patients with EGFR mutation. J Thorac Oncol 2015; 10: 910-923.
[33] Arasada RR, Shilo K, Yamada T, Zhang J, Yano S, Ghanem R, Wang W, Takeuchi S, Fukuda K, Katakami N, Tomii K, Ogushi F, Nishioka Y, Talabere T, Misra S, Duan W, Fadda P, Rahman MA, Nana-Sinkam P, Evans J, Amann J, Tchekneva EE, Dikov MM and Carbone DP. Notch3-

dependent β-catenin signaling mediates EGFR TKI drug persistence in EGFR mutant NSCLC. Nat Commun 2018; 9: 3198.
[34] Zhou J, Wang X, Li Z, Wang F, Cao L, Chen X, Huang D and Jiang R. PIM1 kinase promotes EMT-associated osimertinib resistance via regulating GSK3β signaling pathway in EGFR-mutant non-small cell lung cancer. Cell Death Dis 2024; 15: 644.
[35] Zheng YW, Li ZH, Lei L, Liu CC, Wang Z, Fei LR, Yang MQ, Huang WJ and Xu HT. FAM83A promotes lung cancer progression by regulating the Wnt and hippo signaling pathways and indicates poor prognosis. Front Oncol 2020; 10: 180.
[36] Rashidian J, Le Scolan E, Ji X, Zhu Q, Mulvihill MM, Nomura D and Luo K. Ski regulates Hippo and TAZ signaling to suppress breast cancer progression. Sci Signal 2015; 8: ra14.
[37] Wang L, Shi S, Guo Z, Zhang X, Han S, Yang A, Wen W and Zhu Q. Overexpression of YAP and TAZ is an independent predictor of prognosis in colorectal cancer and related to the proliferation and metastasis of colon cancer cells. PLoS One 2013; 8: e65539.
[38] Li Z, Wang Y, Zhu Y, Yuan C, Wang D, Zhang W, Qi B, Qiu J, Song X, Ye J, Wu H, Jiang H, Liu L, Zhang Y, Song LN, Yang J and Cheng J. The Hippo transducer TAZ promotes epithelial to mesenchymal transition and cancer stem cell maintenance in oral cancer. Mol Oncol 2015; 9: 1091-1105.
[39] Wang Y, Dong Q, Zhang Q, Li Z, Wang E and Qiu X. Overexpression of yes-associated protein contributes to progression and poor prognosis of non-small-cell lung cancer. Cancer Sci 2010; 101: 1279-1285.
[40] Zhao B, Wei X, Li W, Udan RS, Yang Q, Kim J, Xie J, Ikenoue T, Yu J, Li L, Zheng P, Ye K, Chinnaiyan A, Halder G, Lai ZC and Guan KL. Inactivation of YAP oncoprotein by the Hippo pathway is involved in cell contact inhibition and tissue growth control. Genes Dev 2007; 21: 2747-2761.
[41] Hao Y, Chun A, Cheung K, Rashidi B and Yang X. Tumor suppressor LATS1 is a negative regulator of oncogene YAP. J Biol Chem 2008; 283: 5496-5509.
[42] Konsavage WM Jr, Kyler SL, Rennoll SA, Jin G and Yochum GS. Wnt/β-catenin signaling regulates Yes-associated protein (YAP) gene expression in colorectal carcinoma cells. J Biol Chem 2012; 287: 11730-11739.
[43] Xin M, Kim Y, Sutherland LB, Qi X, McAnally J, Schwartz RJ, Richardson JA, Bassel-Duby R and Olson EN. Regulation of insulin-like growth factor signaling by Yap governs cardiomyocyte proliferation and embryonic heart size. Sci Signal 2011; 4: ra70.
[44] Wang M, Zhao J, Chen T, Hu X, Wang L, Shi Y and Liu Y. Efficacy and safety of osimertinib plus anlotinib in advanced non-small-cell lung cancer patients after drug resistance. Thorac Cancer 2023; 14: 873-880.
[45] Zhou B, Gong Q, Li B, Qie HL, Li W, Jiang HT and Li HF. Clinical outcomes and safety of osimertinib plus anlotinib for patients with previously treated EGFR T790M-positive NSCLC: a retrospective study. J Clin Pharm Ther 2022; 47: 643-651.
[46] Xu Y, Qie H, Zhao H, Gao X, Gao J, Feng Z, Bai J and Wang M. Simultaneous determination of icotinib, osimertinib, aumolertinib, and anlotinib in human plasma for therapeutic drug monitoring by UPLC-MS/MS. J Pharm Biomed Anal 2024; 251: 116445.
[47] Yu L, Xu J, Qiao R, Han B, Zhong H and Zhong R. Efficacy and safety of anlotinib combined with PD-1/PD-L1 inhibitors as second-line and subsequent therapy in advanced small-cell lung cancer. Cancer Med 2023; 12: 5372-5383.
[48] Li X, Wang W, Xu C and Yuan Q. Efficacy and safety of immunotherapy combined with anlotinib as first-line treatment in older NSCLC patients with PD-L1 expression < 50. Curr Cancer Drug Targets 2025; 25: 818-828.
[49] Li X, Wu D, Peng Y, Tang J and Wu Y. Efficacy and safety of PD-1/L1 inhibitors combined with anlotinib versus PD-1/L1 inhibitors combined with bevacizumab in second-line treatment of advanced non-small cell lung cancer patients: a comparative cohort study. Curr Cancer Drug Targets 2025; 25: 855-864.
[50] Dong B, Chen L, Pang Q, Jiang O, Ge H, Cheng Y, Zhou R, Meng X, Li J, Zhu X, Wang X, Cao Q, Ji Y and Chen M. TQB2450 with or without anlotinib as maintenance treatment in subjects with locally advanced/unresectable non-small cell lung cancer that have not progressed after prior concurrent/sequential chemoradiotherapy (R-ALPS): study protocol for a randomized, double-blind, placebo-controlled, multicenter phase III trial. Transl Lung Cancer Res 2024; 13: 2828-2837.
[51] Fan P, Qiang H, Liu Z, Zhao Q, Wang Y, Liu T, Wang X, Chu T, Huang Y, Xu W and Qin S. Effective low-dose Anlotinib induces long-term tumor vascular normalization and improves anti-PD-1 therapy. Front Immunol 2022; 13: 937924.
[52] Yin X, Liu X, Ren F and Meng X. The later-line efficacy and safety of immune checkpoint inhibitors plus anlotinib in EGFR-mutant patients with EGFR-TKI-resistant NSCLC: a single-center retrospective study. Cancer Immunol Immunother 2024; 73: 134.

[53] Luo J, Cheng K, Ji X, Gao C, Zhu R, Chen J, Xue W, Huang Q and Xu Q. Anlotinib enhanced CD8(+) T cell infiltration via induction of CCL5 improves the efficacy of PD-1/PD-L1 blockade therapy in lung cancer. Cancer Lett 2024; 591: 216892.
[54] Matarrese P, Vona R, Ascione B, Cittadini C, Tocci A and Mileo AM. Tumor microenvironmental cytokines drive NSCLC cell aggressiveness and drug-resistance via YAP-mediated autophagy. Cells 2023; 12: 1048.
[55] Hong S, Yu N, Cho JY, Lee GK, Ahn BC, Lee Y, Sim H, Song BR, Hwang M, Kim S, Kim JH, Park C and Han JY. VEGF signal complexity confers resistance to atezolizumab, bevacizumab, carboplatin, and paclitaxel in EGFR-tyrosine kinase inhibitor-resistant non-small cell lung cancer. MedComm (2020) 2025; 6: e70335.
[56] Zhang F, Huang B, Xu Y, Cao G, Shen M, Liu C and Luo J. MISP suppresses ferroptosis via MST1/2 kinases to facilitate YAP activation in non-small cell lung cancer. Adv Sci (Weinh) 2025; 12: e2415814.